

Development of Smart Membrane for Leak Detection in Pipeline

by

Trung Viet Nguyen

A thesis submitted in partial fulfillment of the requirements for the degree of

Master of Science

Department of Mechanical Engineering
University of Alberta

© Trung Viet Nguyen, 2016

Abstract

Pipelines are the most important liquid and gas transportation methods in various industries. They help to reduce the cost and to minimize the environmental impacts. However, the public maintains high resistance to pipeline's developments because they are exposed to the consequences of pipeline's leakages. Thus, pipeline operators must aim at zero leakage in their systems for public's safety and also for gaining public support. However, leaks are inevitable due to various reasons, and pipeline operators can only reduce leak consequences by early detections. As a result, many leak detection systems (LDSs) have been developed. According to the study of Afzal, most of those systems suffered from both technical and economical problems when applied to complex pipeline systems. These LDSs systems are optimized to detect different leaks and also to minimize the costly false alarms; thus, they overlook small leaks, i.e. pinhole leaks. This thesis introduces a new LDS that will solve both technical and economic problems. The system includes a flexible membrane with a sensor printed on its surface. This membrane will be wrapped around the 36" pipe to capture the release products. Also, its sensor will detect the membrane's strain created by these products and send the signal to pipeline operators. For the system to be sensitive and cost effective, the membrane had to be optimized to achieve the longest lengths with the predefined thicknesses. Since this technology will be incorporated into the protective wraps, the optimization procedure will use the material properties and the popular thicknesses of the protective wraps.

To achieve the optimum design, the sensors' geometry was optimized first. Then, they were printed on a flexible membrane using a low-cost printer, conductive ink, and resistive ink. The sensors were designed as a half Wheatstone bridge because this setup gave the highest signal outputs under

different loading conditions. The sensors were studied using the four points bending test, and the gauge factors were determined to be 4 and 7.85 for the conductive ink and resistive ink, respectively. Based on this information, a prototype of the membrane was manufactured. This prototype was subjected to the dimple test to evaluate its workability and to compare with the FEA model. Also, the full FEA model of the membrane with the sensor was created. This model was used to optimize the length and thickness of the membrane. The optimum design was achieved when the printed sensor can generate a signal with a signal-to-noise ratio (S/N) of 30 dB under deformation. The simulation indicated that the elastomer membrane with the length of 8.5 ft and thickness of 0.03” can detect pinhole leak on the 36” pipe in 0.8 seconds.

Preface

This thesis is an original work by Trung Nguyen. The research project, of which this thesis is a part, received research ethics approval from the University of Alberta Research Ethics Boards, Project Name “Development of Smart Membrane for Leak Detection in Pipeline”.

The research conducted for this thesis led by Professor Walied Moussa at the University of Alberta. The testing apparatus referred to in chapter 4 was designed by myself. The data analysis in chapter 3 and 4 are my original work, as well as the literature review in chapter 2.

Acknowledgements

I would like to dedicate this Master thesis to my family whose love and supports help me to archive many great accomplishments. I would like to acknowledge the inspirational support and guidance of Dr. Moussa during my study; without him, this thesis would not be feasible. I would also like to thank my colleagues in the lab for providing me with useful resources.

Table of Contents

List of Tables	viii
List of Figures	ix
List of Symbols.....	xiii
Chapter 1: Introduction.....	1
1.1. Motivation.....	1
1.2. Proposed Approach.....	3
1.3. Research Objectives	4
1.4. Thesis Outline	5
1.5. References.....	6
Chapter 2: Background and Literature Review.....	8
2.1. Introduction.....	8
2.2. Pipeline Systems	12
2.3. Leak Detection Systems	13
2.3.1. External Systems	14
2.3.2. Internal System	19
2.4. Pipelines' protective tapes.....	26
2.5. Strain Gauge and Wheatstone bridge	27
2.5.1. Quarter-Bridge	29
2.5.2. Half-Bridge	29
2.5.3. Full-Bridge.....	30
2.6. Conductive ink and Resistive ink	30
2.7. Summary.....	31
2.8. References.....	37
Chapter 3: Design of the Smart Membrane	43
3.1. Design Philosophy	43
3.2. Designs of smart membrane.....	44
3.3. Design of Sensors.....	48
3.3.1. Printed strain gauge design.....	50
3.3.2. Four points bending test	55
3.4. Optimization of the membrane.....	64
3.5. References.....	69
Chapter 4: Evaluation of the membrane prototype	70

4.1. Simulation Setup	70
4.2. Dimple Test Setup.....	71
4.3. References.....	76
Chapter 5: Conclusion and Future Works	77
5.1. Conclusion	77
5.2. Future works	78
References.....	79
Appendix: Simulation Appendix	87

List of Tables

Table 2-1: Comparison between Ultrasonic and MFL PIGs.	21
Table 2-2: Comparison between Conductive 9101 Ink and Resistive 3804 Ink	31
Table 2-3: Summary of LDS methods available and their abilities to detect pinhole leaks.	33
Table 3-1: Comparison between Conductive PSG and RSG.....	56
Table 4-1: Resistance of each printed strain gauge in the Wheatstone bridge circuit.	74

List of Figures

Figure 2.1- Elevated section of Trans Alaska Pipeline [2]	8
Figure 2.2 - Percentage of spills detected by LDS comparing to the other methods [3].....	9
Figure 2.3 - Characterization of Pipeline ROW Leaks [4].	10
Figure 2.4 - Rupture of the pipeline [57].....	10
Figure 2.5 - Local corrosion on pipeline [9].....	11
Figure 2.6 - Acoustic Emission Integrity Diagnostic.	16
Figure 2.7 - Distributed Temperature Sensing System, i.e. Fiber Optic Cable.	17
Figure 2.8 - Leak Detection and Localization Using Vapor Sensing Tube [13].	18
Figure 2.9 - PIGs launcher and receiver station. [30].....	20
Figure 2.10 – Protective Wrap on Pipeline [56].....	27
Figure 2.11- Strain gauge nomenclature	27
Figure 2.12 - Wheatstone bridge circuit with resistors in the conventional order.	28
Figure 3.1 - Two designs of the membrane. The 1 st design localizes the leak by interpolating voltages from multiple sensors. The 2 nd design detects the presence of the leak at the bottom of the membrane.	44
Figure 3.2 - Maximum hoop strain caused by the leak as it moved from the pipe's middle region to end region. This fact indicated that the sensor density of the 1 st design must be varied along the pipe to account for the strain difference.....	45
Figure 3.3 - Hoop strain and axial strain distributed along the membrane under 1 lb of leak substance. This fact indicated that the 2 nd design should measure the hoop strain for the highest signal.	47
Figure 3.4 - Two methods for installing the smart membrane on the pipe.	48

Figure 3.5 - Different Wheatstone bridge installed on the membrane. (Top) Quarter-bridge – Small voltage output, (Middle) Full-bridge – Small voltage output as all sensors experienced tensions, (Bottom) Half-bridge – Highest voltage output.	49
Figure 3.6 - Sample to study the printer's capacity to print long strip. The strips' thickness was 0.039" and their lengths were increased from 0.197" to 1.18".....	50
Figure 3.7 - Multimeter used in the experiment.	51
Figure 3.8 - The resistance changed as the length increased. Notice that the error was also increased with the length. Thus, the printer was not able to print long strips.	51
Figure 3.9 - Printing direction according to the printing mechanism.	52
Figure 3.10 – Testing the consistency of strips' thicknesses and the printing directions. Vertical strips (right) are more resistant than horizontal strips (left).	52
Figure 3.11 - Resistances of the strips printed in horizontal and vertical direction. The uncertainties and resistances of vertical strips were higher than horizontal strips'.	53
Figure 3.12 - (Top) the gaps between the small segments laid down by the printer acted like the resistances in series. (Bottom) close up of the defected strip that was printed horizontally. Horizontal lines with different thickness (dark/light color lines) could be observed.	54
Figure 3.13 - Conductive PSG installed on the steel specimen.	54
Figure 3.14 - Solder paste used to connect the wires to the strain gauges.	55
Figure 3.15 - Circuit for PSG (left), and circuit for RSG (middle), and the Isolated Strain Gauge Input (right).	56
Figure 3.16 - Four points bending test setup.	57
Figure 3.17 - Test specimen with PSG on top and RSG on the back. The lower rig would move up, and it was controlled by a computer.	57
Figure 3.18 - Voltage output from the conductive PSG connected in the Quarter-bridge configuration. The force was from the load cell under the lower rig.	58

Figure 3.19 - Gauge factor of the conductive PSG. The gauge factor was averaged from 03:32 to 03:48 when the specimen was in maximum deformation.	59
Figure 3.20 - Four points bending test setup with Half-bridge PSG installed. The RSG was in Quarter-bridge configuration.	60
Figure 3.21 - Strain calculated from the Half-bridge formed by conductive PSG with gauge factor of 4. Notice that the strain from the RSG was inverted for comparison.	60
Figure 3.22 - Residual strain on the top of the substrate cause the compression.	61
Figure 3.23 - Resistive PSGs installed on the four points bending specimens.	62
Figure 3.24 - Gauge factor of the resistive PSG. The gauge factor was averaged from 02:43 to 02:53 when the specimen was in maximum deformation.	63
Figure 3.25 - The strain from the resistive PSG and the strain from the RSG. Notice that the strain in RSG is inverted for comparison.	63
Figure 3.26 - (Left) Elements Circu124 connect the two meshed strain gauges. (Right) The connection between strain gauges' elements (red) and membrane's elements (violet).....	66
Figure 3.27 - The stress distribution on the membrane. The figure also showed voltage distribution in the strain gauges (the deformation was exaggerated).	66
Figure 3.28 - The S/N varies with thickness and length of the membrane. The S/N of the sensor decreased as the membrane's length and thickness increased.	67
Figure 4.1 - 6 Axis Testing System with Dimple Test rig installed on top.....	71
Figure 4.2- (a) Handle that controlled the perturbation. (b) The locations of the marks used to control the amount of perturbation.	72
Figure 4.3 - The measured perturbations compare to the theoretical perturbations. The measured perturbation was measured using the digital caliper.	73
Figure 4.4 - (Left) Sample of dimple test with PSG, and its dimensions are in inches. (Right) An actual prototype was installed on the dimple test rig.....	73

Figure 4.5 - The setup for the dimple test. 74

Figure 4.6 - The higher and closer the perturbation is, the higher the change in the resistance of the sensor.
The experimental data do not follow simulation data because of the wrinkling membrane. . 75

List of Symbols

Δd : Perturbation (in/mm)

ε : Strain

ε_L : Longitudinal strain

ε_w : Transverse strain

I_{ex} : Excitation Current (A)

LDPE: Low-Density Polyethylene

LDS: Leak Detection System

R: Strain gauge resistance (Ω)

R_f : Resistance of the film (Ω)

PSG: Printed Strain Gauge

RSG: Reference Strain Gauge

ρ : Resistivity (Ωm)

S/N: Signal to Noise Ratio (dB)

V_{ba} : Voltage output from the sensor (V)

ν_f : Poisson ratio of the film

ν_s : Poisson ratio of the substrate

Chapter 1: Introduction

1.1. Motivation

Pipelines are the safest and most cost effective methods to transport crude oil over long distances [1]. Some major pipelines, such as Keystone XL, can reach distances over thousand miles and eliminate thousands of rail cars and tanker trucks on the roads. Despite the environmental and economic benefits, the publics still persist high resistances to the developments of pipelines, for instance, the postponement of Keystone XL phase 4. The publics' main concerns come from their negative experiences with pipelines' leaks. For instance, on July 25th, 2010, Enbridge Line 6B leaked in Marshall, MI for 17 hours before it was detected. A large amount of diluted bitumen gushed into the Kalamazoo River and damaged the local water resource. Besides affecting publics' safeties, the financial cost of this incident was exceeded \$820 MM [2] including 3.7 MM in fines [3]. The financial costs associating with pipelines' failures are usually complicated. Furness and Van Reet suggested that these costs could be divided into four main areas [4]:

- Losses of lives and properties
- The loss products and downtime of the systems
- Environmental cleanups
- Fine and legal suits

As a result, pipeline operators always aim to minimize these financial and social costs through early leak detections and frequent inspections.

Pipeline leaks are defined as the losses of pipeline's products to the environments while the pipelines are in operations [5]. Pipeline leaks are caused by various factors, and these factors can be categorized into four classifications [4]:

- Pipeline corrosion
- Intentional damage
- Unintentional damage
- Operation outside design limits

Pipelines are subjected to both internal and external corrosions during their service periods. Internal corrosions usually affect pipelines that carry corrosive products, or pipelines that are left partially full for periods of time [6]. External corrosions occur because pipelines are exposed to the corrosive environments such as moisture, and galvanic effects of the surrounding soil [6]. Leaks also occur if pipeline operators exceed the design limits, such as over-pressuring the pipes. Leaks caused by these reasons usually occur at the weak spots in the pipe systems, for instance, joints, flanges, and valves. Intentional or unintentional damages are usually caused by third-parties. These third parties usually report damages to the pipeline operators directly. Thus, they are not as dangerous as the other damages' types.

Pipelines' leaks are characterize based on their sizes ranging from the smallest size, i.e. pinhole leaks, to the complete failure, i.e. ruptures. Pinhole leaks are considered the most dangerous because they often occur unnoticeably over a long time [7]. If these leaks occur unnoticeably, they will grow into bigger sizes after damaging the surrounding environments. Nowadays, pipeline operators rely on Leak Detection Systems (LDSs) as their first lines of defense against leaks. Various LDSs with different detecting mechanisms have been used in the industry. However, they are complex, expensive, lacking redundancy, and not reliable for pinhole leaks detections. Most of the current LDSs often misinterpret pinhole leaks as environmental noises, and they do not give them the appropriate attentions and treatments. The reason is that current LDSs are optimized to minimize the costly false alarms, thus, they are insensitive to pinhole leaks. Despite the fact that LDSs' manufacturers claim that their systems can detect pinhole leaks, most pinhole leaks are detected by the pipeline's employees or people at the scene [8]. These leaks are only detected after their damages become observable and require millions of dollars to recover.

The work in this thesis will focus on bridging the gap between technical challenges and economic problems. The research will develop a new pinhole LDS which is sensitive, low-cost, and can be incorporated into the existing pipeline systems.

1.2. Proposed Approach

The flow rates of pinhole leaks are relatively small, and they can be misinterpreted as environmental noises. Thus, it is challenging for current LDSs, which are optimized to detect bigger leaks, to detect this type of leak. However, if all the leaked products are collected, they will create a high signal that can be detected easily. This thesis suggests that pipeline operators should wrap their pipes with the smart membranes. Each smart membrane consists of a flexible elastomer sheet with strain sensors installed on its surface. The membranes will collect leaked products and deform under the leak products' weights. The strain sensors, which are strain gauges connected in Wheatstone bridge, on the membranes will detect these deformations and send signals to pipeline operators. These membranes work best on the elevated pipelines because they are free to deform. However, they can be used on underground pipelines if drains are created under the buried pipes. These drains give spaces for the membranes to deform. Wrapping pipelines to protect them from corruptions has been a standard in the industry, therefore, the addition of those smart membranes is feasible. Smart membranes can also be deployed on existing pipelines with appropriate wrapping technologies.

With the development of the printed electronics technologies, it is possible to print sensors for various applications. These sensors usually consist of conductive and resistive elements that are positioned to sense strains in specific directions. The advantages of these sensors are that they can be printed on flexible materials in a short time. They are more sensitive and inexpensive comparing to the conventional sensors [9]. As a result, printed sensors are ideal candidates for smart membranes where high sensitivity and low production cost are important.

The process of designing smart membrane started with a study on the printer's capacities. Multiple lines were printed to study the inks' resistances, accuracy, and precision of the printer. The information was used to design strain gauges that had high and consistent resistances. These strain gauges were evaluated using four points bending test to determine their gauge factors and limitations. After that, a prototype of the smart membrane was created and evaluated. In order to replicate

actual loads that the membrane experiences, the dimple test was developed and used for evaluating the prototype. A simulation model of this prototype was also created to compare to the actual dimple test. This step was crucial because it connected the real membrane to the simulation model which was used to optimize the membrane's geometries. After correlating the results from the simulation model and dimple test, the simulation model was used to optimize membrane's geometries. Since the membranes were expected to be similar to the protective wraps, their dimensions and materials must be the same. Thus, the optimization procedure will focus on finding the optimum membrane's geometries based on the information from the current protective wraps.

1.3. Research Objectives

The research in this thesis has a number of objectives, including:

- There are multiple setups for the Wheatstone bridge, including Quarter-bridge, Half-bridge, and Full-bridge. Each bridge setup has its advantages and disadvantages. Thus, the first objective is to predict the loading conditions on the membrane and to design the Wheatstone bridge that can detect the strains in these loading conditions.
- Different printing techniques and inks result in strain gauges with different gauge factors. The second objective is to design and to print the strain gauges that are consistent and sensitive. After this objective is achieved, a prototype membrane with similar strain gauges can be printed.
- The third objective is to design and manufacture a testing rig to evaluate the prototype. This system, referred as Dimple Testing Rig, should be designed so that it evaluates the membrane without knowing the membrane's material.
- The next objective is to create a simulation model for the membrane prototype. The voltage outputs from this model must be similar to the voltages from dimple test. After the fourth objective is achieved, the simulation model will be modified so that it is similar to the actual membrane.

- The final objective is to optimize the membrane's length and thickness so that, as the leak occurs, the membrane will create a signal with S/N of 30 dB. The membrane should also detect the leak in less than one minute so that it has competitive advantages over other LDSs.

1.4. Thesis Outline

The thesis is divided into six chapters. The first chapter is an Introduction that consists of the Motivation, Proposed Approach, and Objectives. Chapter 2 will review all technologies and materials relevant to the research. Chapter 3 will discuss the design of strain gauges in the sensor, and the experiment to study these strain gauges. Chapter 4 will be about the design of the Dimple Testing Rig, the Dimple Test, and the confirmation of the FEA model. Chapter 5 will consider the optimization process, the final design of the membrane, and the suggested installation methods. The last chapter will be a conclusion to evaluate whether or not the objectives were achieved.

1.5. References

- [1] CEPA, *Liquids Pipeline* [Online]. Available: <http://www.cepa.com/about-pipelines/types-of-pipelines/liquids-pipelines>.
- [2] C. Kelly. (2013). *Enbridge Cleanup May Cost \$1-billion, Company Warns* [Online]. Available: <http://www.theglobeandmail.com/globe-investor/enbridge-cleanup-may-cost-1-billion-company-warns/article10041757/>.
- [3] Reuters. (2012). *Update 2-Enbridge Fined \$3.7 Mln for 2010 US Oil Spill* [Online]. Available: <http://www.reuters.com/article/enbridge-spill-fine-idUSL2E8I2DTH20120703>.
- [4] R. Fletcher, and J. V. Reet, *Pipeline Rules of Thumb Handbook: A Manual of Quick, Accurate Solutions to Everyday Pipeline Engineering Problems*, 7th ed., Amsterdam: Gulf Professional Publishing, 2009, pp. 605-614.
- [5] EUB, "Pipeline Performance in Alberta, 1990-2005," Alberta Energy and Utilities Board, Calgary, 2007.
- [6] C. Cheng, "Evaluation of Pipeline Leak Detection Technologies," M.Eng. thesis. Dept. Mech. Eng., University of Alberta, Edmonton, 2013.
- [7] A. Swift. (2011). *The Keystone XL Tar Sands Pipeline Leak Detection System Would Have Likely Missed the 63,000 Gallon Norman Wells Pipeline Spill* [Online]. Available: <https://www.nrdc.org/experts/anthony-swift/keystone-xl-tar-sands-pipeline-leak-detection-system-would-have-likely-missed>
- [8] L. Song. (2012). *Few Oil Pipeline Spills Detected by Much-Touted Technology* [Online]. Available: <http://insideclimatenews.org/news/20120919/few-oil-pipeline-spills-detected-much-touted-technology>.

[9] A. Jager A. et al., "Investigation on Strain Gauges Made from Carbon Black Based Ink," in *AMA Conferences*. 2015.

Chapter 2: Background and Literature Review

2.1. Introduction

Pipelines are the most important infrastructures for moving liquid and gas over long distances. Transporting those substances by rail or tanker trucks is not economically feasible [1]. Using pipelines instead of trucks also reduces the carbon footprint on the environment [1]. Pipelines can be constructed underground, elevated above ground, or a combination of both. For example, Trans Alaska Pipeline has 420 miles of its 800 miles length built elevated on the ground [2].



Figure 2.1- Elevated section of Trans Alaska Pipeline [2]

Even though pipelines are good for the economy and the environment, their developments usually face enormous publics' resistances, such as the development of Keystone XL project. These resistances come from the fears that leaked products will damage the surrounding environments and publics' safeties.

Kiefner and Associates examined 759 leak incidents between January 1, 2010, and July 7, 2012, from the U.S. Department of Transportation Pipeline and Hazardous Materials Safety Administration and pointed out that 562 out of 759 incidents occur in the operators' facilities. These facilities consisted of complex elevated pipes with pumps, valves, and flanges that were considered to be weak spots on pipelines. These facilities were manned by pipeline operators; thus, leaks happened in these

locations were detected early and not publicly dangerous. On the other hand, 197 of the 759 incidents occurred on the pipeline right-of-way (ROW) and cause significant damages to the environments. These leaks also threatened publics' safeties, and thus they usually draw publics' attentions. Due to these reasons, LDSs' manufacturers often focus on the ROW areas.

Detecting leaks in the ROW regions is challenging because it is lengthy and located in the remote regions. According to Kiefner's report, the average leaked volumes at the ROWs are 29,230 gallons compared to 5,588 gallons on the facilities' regions. This fact indicates that response time at the ROW is significantly longer than the response time at the pipeline facilities. In fact, most of the leaks at the ROW are detected by the publics [3].

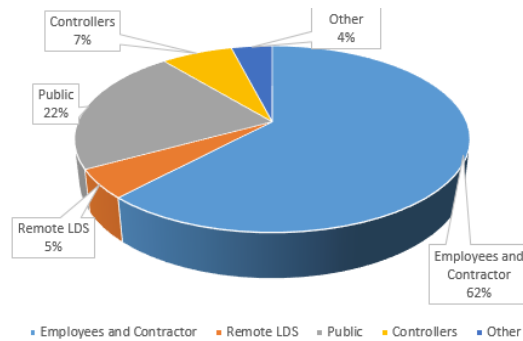


Figure 2.2 - Percentage of spills detected by LDS comparing to the other methods [3].

Leaks could occur on any parts of pipelines. Kiefner analyzed that out of the 197 leaks on ROW, 132 of them are from the pipes' bodies, 17 from the valves, 5 from flanges, and 43 from the others. Figure 2.3 shows the breakdown percentages of leaks on pipelines

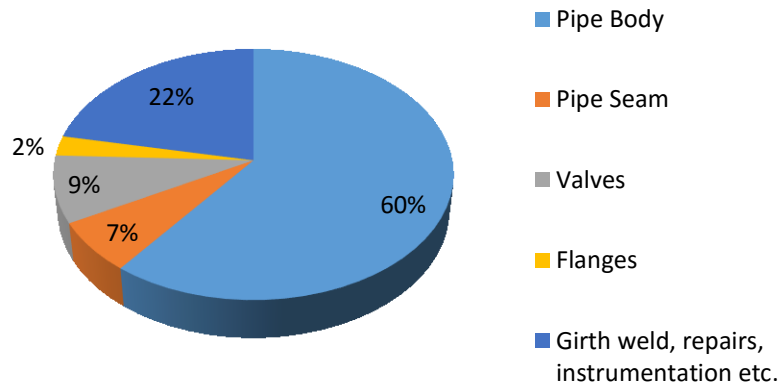


Figure 2.3 - Characterization of Pipeline ROW Leaks [4].

Pipeline leaks are defined as the releases of pipelines' products into the environments. While there are no standard definitions of pipeline leaks, they are often classified into ruptures, holes, and pinholes/cracks based on their sizes [5]. Rupture failures are defined as holes which have diameters greater than the pipelines' diameters. This release type often impairs the operation of the pipeline, thus, it triggers responses quickly.



Figure 2.4 - Rupture of the pipeline [57].

Ruptures can be fixed by replacing the ruptured segments. This process strongly affects the operations of pipeline systems. After rupture failures, holes are defined as the medium leaks which are smaller than ruptures and bigger than pinholes. Holes usually have their diameters between 20 mm to the pipes' diameters. This type of release occurs most often and does not impair the pipeline operations [5]. Because of their frequent occurrences, holes attract the attentions of pipeline operators and LDS companies from the other leak types. These medium leaks can be fixed by various methods ranging from covering the leaks with composites to replacing the

whole pipe segments. Finally, pinhole leaks have diameters smaller than 20 mm and were caused by local corrosions on pipelines [6]. This type of leak has the discharge rate of 1% to 1.5% of its volume flow rate [7]. This small percentage flow rate is equivalent to a lot of releases because of the high flow rate in the pipeline. In addition, this type of leak can occur unnoticeably for a long time, and the leaked products can accumulate to cause significant losses and damages. Detecting this leak type is challenging because their released products, i.e. their indications, are relatively small. These leaked indications are often misinterpreted as environmental noises, and therefore, pipeline operators may not detect them until they cause significant damages. The dangers of this type of leak can be observed in the Amoco Oil leak on August 17, 2010, in which 38,640 gallons of gasoline released into the environment. The leak was detected by the emergency responder who smelled the leaked products in the sewer drains. Even though this pipeline was equipped with both Supervisory Control and Data Acquisition, i.e. SCADA, and Computational Pipeline Monitoring, i.e. CPM, neither of them detected nor confirmed the leak [8].



Figure 2.5 - Local corrosion on pipeline [9].

Pinhole leaks can be fixed using either composite materials or the pinhole leak repair clamps. Due to the dangerous of pinhole leak, this thesis will introduce a new low-cost LDS system that is able to detect the pinhole leak.

2.2. Pipeline Systems

Pipelines are the main transportation systems for oil and gas industries. According to the Interstate Natural Gas Association of America (INGAA), there are 542,500 miles of pipelines will be installed between now and 2035 to transport oil and gas from a projected 1.2 million new wells [48]. The total distance of these pipes is even longer than a round trip to the moon.

Pipelines are used to transport three types of fluids: oils, natural gas, and hazardous liquids. Oils include various types of hydrocarbons. These oils are different in their properties, such as specific gravities, acidities, viscosities, etc. Natural gasses include mainly methane, ethane, propane, butane, and sulfur gasses. Hazardous liquids usually include the products refined from crude oil, for instance, gasoline, diesel, natural gas liquids, and saline wastewaters. Pipeline networks can be divided into three parts: gathering, transmission, and distribution. Gathering pipelines are small, their diameters range from 2 to 12 inches [49] [50]. These pipes are used to transport the fluid from wells to transmission pipelines. Transmission pipelines are often referred as “interstate highways” in pipeline systems. They are largest and longest pipes that have diameters of 16 to 48 inches [51] [52]. They transport hydrocarbons to the processing plants or storages. The last type of pipe is the distribution pipeline that has various sizes. These pipes are used to deliver hydrocarbons directly to the end consumers such as individual homes or business customers.

Most of the pipelines are made of carbon hardened steels. This type of material is used because it can be welded easily. It is also capable of withstanding high temperatures and pressures. Moreover, it can be protected from corrosion caused by the fluids it carries. The fluids are pushed through the pipes using pumps at pump stations (for liquids) or by compressors (for natural gas). In the transmission pipelines, these fluids are pressurized at 600 to 1400 psi so that they can be transported through long distance [51] [52]. Pipeline systems are also equipped with shutoff valves, which are located every 5 to 20 miles apart, to stop the flows in cases of emergency or maintenance [52][53][54].

2.3. Leak Detection Systems

Various LDSs are currently used by pipeline operators to maintain the safeties of their systems. These systems may vary significantly in their performances and their costs. To reduce the installation complexity, some systems rely on the field equipment of the pipelines to collect data. The candidates for these systems are the internal LDS, such as Real Time Transient Method or mass/volume balance methods. On the other hand, some systems require external sensors or equipment to monitor the integrities of the pipeline systems. The examples of this systems are smart pigging, acoustic emission detectors, and fiber optic cable. Thus, to categorize the LDSs, they are divided into two main catalogs: external system and internal system [10]. Most of the pipeline operators use both internal and external LDSs in conjunction to add layers of redundancy and improve their detected rate.

The performances and integrities of most current LDSs are dependent on various factors, such as fluid types, pipeline routes, surrounding environments, and operation techniques. To evaluate the feasibility of LDSs before installing it on the systems, pipeline operators usually consider the criterions below [11]:

- LDS Principle: how the LDS operates.
- Application requirements: requirements the LDSs need to operate.
- Fluid property: properties of the fluid, for instance, gas, liquid, or a mixture of both.
- Reliability: the ability of the LDSs to avoid false alarms during normal working conditions.
- Sensitivity: the ability of LDSs to detect small leak size in a short time period.
- Robustness: the ability of LDSs to operate in any situations, even with the loss of some measuring instruments.
- Leak location accuracy: the ability of LDSs to accurately localize the leak.
- Calculation of Leak Size: the ability of LDSs to estimate the leak's size based on the information it collected.
- Installation cost: the cost of installing the LDSs.

- Maintenance cost: The cost of maintaining the LDSs.

It is important to notice that there are no clear government's requirements for LDSs [4]. In Canada, the Annex E in CSA Z662-11 only recommends the practices for liquid hydrocarbons, and these recommendations are not mandatory. Similar to Canada, the U.S. Department of Transportation and Pipeline and Hazardous Materials Safety Administration does not apply strict regulations on LDSs [4]. It is the responsibilities of pipeline operators to establish the tolerances for their systems. As a result, most pipeline operators optimize their systems to minimize the false alarms. This fact makes detecting pinhole leaks a challenge for most pipeline operators.

2.3.1. External Systems

External LDSs are systems that detect the present of pipeline's products, by different means, outside of the pipelines. These systems involve additional sensors and instruments installed along the pipes. Thus, these systems require high installation costs, and they are better suited for short pipeline segments [12]. The advantages of those systems are that they can be easily incorporated into most pipeline systems while not interfering with their operations. They also provide very accurate leak localizations at the expense of high installation costs [13].

2.3.1.1. *Intermittent Methods*

Intermittent methods are considered to be one of the most basic techniques in external LDSs. These methods involve periodical inspections on pipelines by various instruments and means such as helicopters, employers, and dogs.

Aerial inspections involve inspecting the pipelines from helicopters. The helicopters are equipped with detection systems such as infrared cameras or leak sniffers. The method is commonly used to detect gas leaks as sensors are capable of looking at infrared spectral signals using nondispersive gas filter correlation techniques. The sensors can also be integrated with other LDSs to provide continuous monitoring of the pipeline systems. The disadvantages of this technique are that it can only be used on short segments pipes, and its accuracy relies on the weather conditions. In addition, the accuracy of this method is higher for the

elevated pipelines comparing to the underground pipelines [14]. For short pipeline segments, pipeline operators deploy their employees to walk along the pipes and do visual inspections. This inspection method can be used to detect pinhole leaks if there are accumulations of leaked product or observable damages on sites. The employees typically look for [15]:

- Stains on pipelines.
- Oil on water's surface.
- Third parties' damages.
- Debris in the ROW.
- Dead vegetation.
- Nearby construction sites.
- Suspicious activities.

2.3.1.2. Acoustic Emission Detectors

This method is one of the most developed LDSs. It is based on the phenomenon that leaked products create acoustic signals of specific frequency ranges as they pass through the leaks. Acoustic sensors installed outside the pipes will continuously monitor these specific frequencies while filtering out the internal noises. As leaks occur, low-frequency signals will be sent and received by the sensors. These signals are analyzed, and alarms will be triggered if the signals fall within the predefined ranges. The acoustic sensors can be located 20 miles apart, but the long distances will reduce their sensitivities [4]. Since the acoustic signals are stronger near the leak holes, localizing the leak is possible by interpolating the signals' amplitudes.

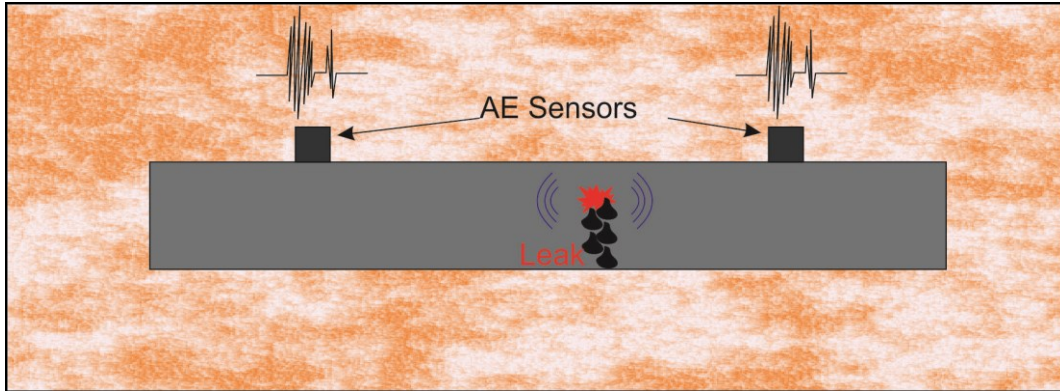


Figure 2.6 - Acoustic Emission Integrity Diagnostic.

The primary drawback of acoustic sensors is that the leak signals can be drowned by environmental noises. In addition, starting and stopping of pumps along the pipe can generate acoustic signals that are similar to leak's signals, thus, numerous false alarms occur with this method. As a result, both mechanical techniques and analysis techniques have been developed to increase the sensitivity of this method while reducing the false alarm rate. The mechanical techniques include injecting air bubbles or solid particles into the fluids to increase the leak signals' amplitudes [17]. On the other hand, analysis techniques can be correlation analysis [18] [1], statistical analysis [19], ANN [20], fuzzy system method [21], frequency analysis [22], and harmonic wavelet analysis [23].

2.3.1.3. Fiber Optic Sensing Cables

Sensing using fiber optics has been developed for decades. While the design's purpose of optic cables is for communications, they can also be used for sensing and measurements. This sensing method utilizes temperature sensitive fiber optic cables that run along the pipes. The optical cables can be buried underground in case of the underground pipelines. When leaks occur, leaked products will come into contacts with the cables and change the temperatures of the cables. For liquid pipelines, the fluid temperatures are usually higher than the surrounding temperatures, thus, the increases in temperature will be detected if the leaked fluids come into contact with the optical cables. The optical cables use Raman backscattering principle to detect these increases in temperatures. Pulsed lasers are coupled into the optic cables and send out light beams. Because of the interactions

between photons and cable's molecules, there will be backscattered lights reflected back. As leaks occur, the fluids come into contact with the cables and changes the cables' temperatures and, subsequently, the backscattered light spectrums. By continuously analyzing these spectrums, the leaks can be detected and localized [24].

The optical cable manufacturers claim that their systems have the resolution of 0.1°C and spatial resolutions of 1 m at the range of 30 km [25]. They also indicate that their systems are able to detect leaks of 10 liters/hour in one minute under controlled environment [25]. In addition to the ability to detect temperature change, fiber optic cables can also detect the strains and vibrations. Therefore, they can be used to detect the disturbances at the ROW regions before leaks occur [26].

Fiber optic cables should be buried below but not directly in contact with the underground pipelines. This position maximizes probability for the optical cables to contact the leaked products that are under gravitational effects.

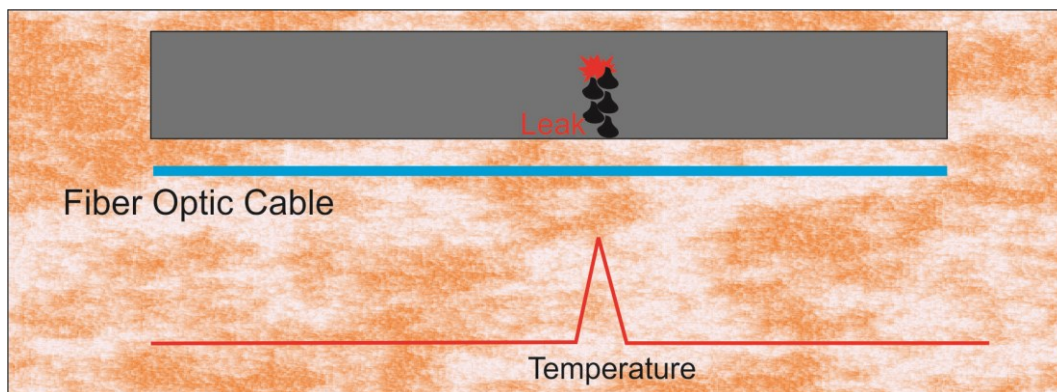


Figure 2.7 - Distributed Temperature Sensing System, i.e. Fiber Optic Cable.

However, this location will prevent leaked products to contact with the cables if the cables locate at or below the water level. The leaked product will rise to the surface rather than sink to the buried cables. To solve this problem, the cables are advised to be positioned above the pipeline if the pipes are below water level [28]. The advantages of optical cables are that they are insensitive to the change in fluid properties as well as the transient stages. They can localize the leak accurately in a relatively short time. On the other hand, the installation processes are expensive and

complex because the locations of optical cables are critical to their abilities to detect the leaked products. In addition to the cost, optical cables are vulnerable to ambient temperatures and moistures, thus, they are also highly susceptible to false alarms. Moreover, this method is also lacking redundancy; the whole system will be disabled if the cables' sections are separated at one location.

2.3.1.4. Vapor Sensing Tubes

If optical cables use temperature differences to sense the leaks, vapor sensing tubes sniff the released products to detect the leaks. In this method, vapor permeable tubes, which are filled with inert gasses or left empty, will be installed along the pipes. These tubes have to be permeable to the vapors from the hydrocarbon fluids that the pipes are carrying. Pumps will push the air inside the tubes at constant velocities to the gas chromatography, which are designed to detect hydrocarbons. The electrolytic cells located close to the pumps' ends inject specific test gasses prior each pumping action. The test gasses are used as markers to localize the leak.

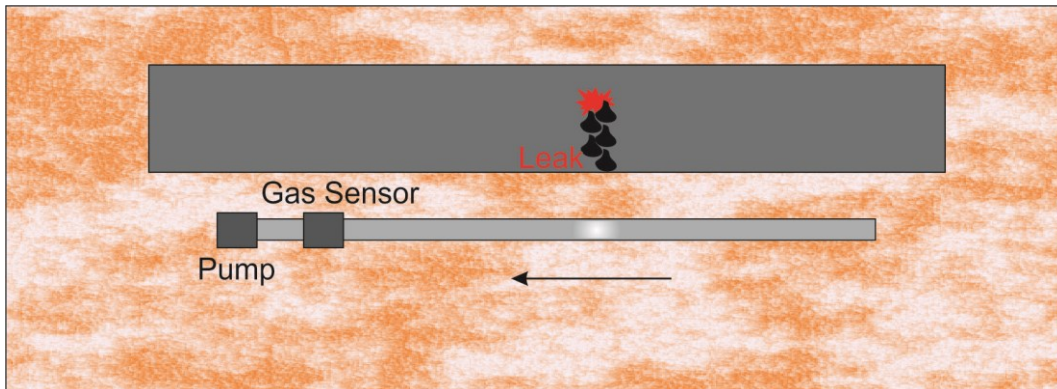


Figure 2.8 - Leak Detection and Localization Using Vapor Sensing Tube [13].

As leaks happen, the leaked vapors will contact with the tubes and, subsequently, diffuse into the tubes due to concentration gradients. This fact generates leak signals in the form of vapor concentrations inside the tubes. Also, the concentrations of vapor are proportional to the leak sizes. After a period of time, the test gasses are injected, and the pumps push air in the tubes with constant velocities past the detection systems. Based on the concentrations and differences in time the peak signals are received by the detectors, the leaks can be detected and accurately

localized. Vapor sensing tubes are highly sensitive and reliable because they require the occurrences of hydrocarbon vapors to generate the alarms. However, background hydrocarbons can accidentally interfere with the systems, and they are the only source of false alarms [13].

2.3.1.5. *Liquid Sensing Cables*

This technology is similar to the vapor sensing tubes discussed before. The specialize cables, similar to optical cables and vapor tubes, are buried close to the pipes. The cables' cores are made of alarm signal wires, the continuity wires, and two sensor wires. The cores are covered by conductive polymer layers that swell when contacting with hydrocarbon substances. The outermost layers are Halar braids that restrict the polymers from swelling outward [29]. Without the leak, the receivers will continuously receive reflected "safe signals". As leaks occur, the wires swell and push the alarm wires. This fact causes impedances' changes and triggers leak alarms. The downside of this technique is that the cables must be replaced after they detected the leaks. In addition, the response times are slow as the conductive polymers need time to swell, and the cables cannot approximate the leak's sizes. Current researches on this technology also indicate that it is not suitable for long pipelines [4]. Similar to vapor sensing cables and optical cables, this technology is suffered from complex installation processes because the cables need to be placed below or above the pipes depending on the environments.

2.3.2. Internal System

Internal LDSs consist of any systems that use flows and pressures inside the pipes to detect leaks. These systems are widely used in the industries because they can be deployed easily to most pipelines. Most of the internal systems utilize the existing pipelines' infrastructures such as flowmeters or pressure-meters. The costs of those systems are difficult to be evaluated because they may not include the instruments on the fields. The internal LDSs usually have three main drawbacks [8]:

- They depend on the qualities and accuracies of field instruments. Internal LDSs will not be able to detect the leak smaller than 1% of flow if they use 1% accuracy meters.

- They may generate false alarms during transient stages of pipelines.
- The thresholds for the leak alarms are defined arbitrarily to minimize the false alarms. If pipeline operators optimize their systems to detect leaks that are more than 1% of flow rate, their systems will be blind to pinhole leaks.

With those drawbacks, current internal LDSs cannot detect pinhole leaks. In fact, Kiefner defined “small” leaks as leaks that cannot be detected by internal systems [8].

2.3.2.1. Pipeline Inspection Gauge (PIG)

Pipeline Inspection Gauges or PIGs are devices inserted into the pipeline systems to perform various tasks such as cleaning the pipe’s inner surfaces or detecting leaks. This method is special because it is the combination of internal and external methods. The PIGs are inserted into pipelines through the PIG launchers, and they will perform multiple tasks inside the pipes without shutting down the systems. At the end of their tasks, they will be taken out from the systems at the PIG receiver stations



Figure 2.9 - PIGs launcher and receiver station. [30]

Cleaning PIGs come in various shapes and designs, and they are employed similar to the other PIGs. On the other hand, inspection PIGs are more complicated comparing to the cleaning PIGs. These PIGs are used to gather information about the pipeline’s integrities as they travel through the pipes. These PIGs have several sensors attached to their bodies, and they will follow the fluid’s flow inside the pipes without interrupting the flows. Two main sensor types are used in the inspection

PIGs: Magnetic Flux Leakage (MFL) and Ultrasonic. MFL PIGs use the on-board permanent magnets to temporarily magnetize the pipes' walls. The changes in the magnetic fields are recorded for analyzing. If the defects, such as pitting, corrosion, or damage present, the magnetic flux will be distorted beyond the walls of the pipes, and these distortions can be evaluated for potential damages [30].

Ultrasonic PIGs emit ultrasonic pulses that travel through the pipes' walls and reflect back as they reach the outer walls. Based on the reflection times, the wall's thicknesses can be measured with the accuracy of +/- 0.4 mm [31]. Since Ultrasonic PIGs using ultrasonic pulses, they require good mediums between the PIGs and the pipes. As a result, Ultrasonic PIGs work best in liquid pipelines. The comparisons of those two PIGs are mentioned by Hodgman [32]

Table 2-1: Comparison between Ultrasonic and MFL PIGs.

Ultrasonic	MFL
<ul style="list-style-type: none"> • Requires a fluid batch for gas pipe • Direct measurement • Tends to be best at detection of defects less than 60% of pipe wall • Generally works best on pipelines with a wall thickness greater than a half inch • May not detect corrosion damage or accurately measure depth of corrosion pits • Requires the removal of internal scale in order for ultrasonic sensors to work properly 	<ul style="list-style-type: none"> • No fluid batch required for gas pipe • Indirect measurement • Tends to be best at detection of defects greater than 30% of pipe wall • Generally works best on pipelines with a wall thickness less than half of an inch • May not detect corrosion pitting less than 30% of the pipe wall • Not as sensitive to internal scale as Ultrasonic tool • Due to measurement accuracy limitations, its ability to

<ul style="list-style-type: none"> • Best tool for monitoring corrosion rate and detection internal corrosion activity 	monitor corrosion rate is limited.
---	------------------------------------

The main advantage of PIGs is that they are cost effective. They can be used to avoid the need for hydro-tests, which will stop the pipeline’s operations completely. Also, they are effective tools for monitoring the metal loss in pipelines [32]. This method’s drawbacks are that it requires infrastructures to inject/receive the PIGs into/from the pipes, and also the pipes must have constant diameters. Moreover, it is not sensitive to internal corrosion damages if the damages are less than 30% of the pipe’s thickness [32]. The biggest disadvantage of this method is that it generates terabytes of data that need to be analyzed by experienced operators. The data analysis can take up to nine months [55].

2.3.2.2. *Volume Balance Method*

This method is one of the popular methods in the internal LDSs. It operates based on the differences in volumes in and out of the pipes. The leak alarms will be generated if there are significant differences in those volumes. Since the flows inside the pipe change under different operation phases, the control operators have to make predictions that the volume differences come from the leaks or from the pipes’ operational conditions. This process will get complicated for pipelines that have multiphase substances or pipelines with complex geometries. As a result, this method is not reliable in detecting leaks during the pipelines’ start-up and shut down stages. This method is also insensitive to the small leaks as the leak’s volumes are too small to be detected by field infrastructures.

2.3.2.3. *Pressure monitoring*

This method compares the pressures and flow rates with the standard data. As the leaks happen, they will create changes in pressures and flow rates inside the pipes, thus, they create deviations from standard pressures and flow rates. The deviations will trigger the leak alarms. There are two ways to detect the deviations: the Negative Pressure Monitoring Method and the Pressure Point Analysis.

- Negative Pressure Monitoring

In the Negative Pressure Monitoring method, the pressure transducers will be installed along the pipes to detect negative pressure drops, Δp , caused by the sudden appearances of the leaks. These negative pressure drops will propagate with the speed of sound in both upstream and downstream directions. This method can also localize the leaks by comparing the differences in time between the upstream and downstream negative pressure waves. In order to capture this wave, this method requires high sampling frequency. The study shows that sampling frequency of 60 Hz is necessary to capture the leak signal. This fast sampling frequency is the main reason that creates two separate technologies based on this method.

The first technology was developed in the early 80's when systems' bandwidths were limited. A large amount of data, which were generated by the high sampling frequency, had to be processed on the site by local processors. If the local processors detected the leaks, they would send signals to the master processors. The master processors would combine different events and time stamps to predict the leaks' presents. If different pressure drop events occurred due to the transient stages, the master processor could mistakenly trigger the leak alarms [11]. In the last few years, the bandwidth problem was overcome, and the new technology based on this method developed. The data were sent directly to the central server for analysis. At this server, the data were filtered and arranged into 3-dimensional maps that indicate different leak and theft events.

The disadvantage of this method is that the sensors only have one chance to detect one pressure drop. If the sensors miss the negative wave, they will not be able to detect the leak. Another disadvantage is that this method cannot locate the creeps or small leaks as the negative pressure waves are small and dominated by noises [33]. The advantages of this method are that it can be employed on existing pipelines easily. It also does not suffer from the changing fluid properties and irregular flow behaviors. Finally, it can detect and localize the leaks in a short time with high accuracy.

- Pressure Point Analysis

The Pressure Point Analysis (PPA) is based on the pressure drop generated by the leak. The PPA method detects leaks by monitoring the pipelines' pressures at points along the pipes and comparing them against statistical trends from the previous measurements [34]. The details of this mechanism would be described in the section below. The disadvantage of this method is that it requires the pressures remain constant in the pipes. Thus, this method may generate false alarms in the transient states of the pipelines.

2.3.2.4. *Statistical analysis*

Statistical analysis is the mechanism that the above LDSs used to detect the leaks. The PPA is one of the commercially available systems. In PPA, the pressure data from the measurement points are compared to the standard data. The Student-t-statistics are used to determine if the measured data are significantly different from the standard data. As the measured data decrease with a level of confidence, the leak alarms will be triggered [11]. The other commercially available analysis is the Sequential Probability Ratio Test (SPRT). This analysis uses statistical processes from decision theory to detect the leaks. Two hypotheses, leak and no-leak, are evaluated. The data used for this evaluation come from the inventory compensated volume balance. By calculating the ratio of the probability of a leak over the probability of no-leak, it decides if the corrected volume balance has increased with a predetermined probability [11]. In order to account for other operating conditions, flow and pressure analysis will be carried out, and their results will be used as factors in the decision schemes. Since the SPRT can be modified to perform in the transient stages, industry has moved towards it rather than the PPA based technology. The applications of SPRT can be seen in pipelines transporting crude oil, multi-product, slurry, ethylene, LPG, natural gas, hydrogen, carbon monoxide, and chlorine [11]. Generally, the advantages of systems using statistical analysis are [11]:

- They are cost effective. As internal LDSs, they often use the existing instruments on the fields.
- They have low false alarm rate.

- Some analysis, for example, SPRT, can work under transient stages.
- The measuring instruments can locate far from others.
- The analysis can estimate leaks' sizes and leaks' locations.
- They are insensitive to changes in fluid properties and ambient conditions.

The drawbacks of LDSs using statistical analysis are

- They depend on the instruments' qualities.
- They are not effective in localizing small leaks.
- They are insensitive to multiple leaks on one pipeline.

2.3.2.5. *Real-Time Transient Model (RTTM)*

RTTM systems are widely accepted as the mature LDSs. It works based on the assumption that the fluid flows in pipelines can be modeled accurately. RTTM uses measured data from pipelines' instruments and SCADA systems to simulate the hydrocarbon flows in real-time. This method involves solving the set of three partial differential equations: continuity equation, momentum equation, and energy equation. Those three equations have no analytical solutions; therefore, they can only be solved using numerical analyses. Also, this method requires extensive configuration of pipeline parameters such as length, diameter, wall thickness, route topology pipeline roughness, pumps, valves, equipment location [11]. When combining with the equation of states, RTTM can solve for the transient states such as start-up and shutdown states of a pipeline [35]. RTTM systems can detect leaks in several ways, the two common ones are [11]:

- Deviation analysis: the system will take measurements from SCADA systems and compare them with the simulated value. If the differences go above the threshold values, leak alarms will be generated.
- Model compensated volume balance: RTTM systems calculate the inventories in real-time. The inventory changes are used to correct the volume imbalances. If the imbalances go above the threshold values, leak alarms will be generated.

The advantages of RTTM systems are that they are cost effective since they use data from existing equipment and SCADA systems. However, RTTM systems still require additional information from the flow such as density, temperature, and viscosity [11]. Since RTTM systems simulate the flows in real time, the other information of this flow can be extracted. For instance, the systems can predict the pressure profiles or track the PIGs. The systems are also able to estimate the leaks' sizes and localize the leaks' positions.

On the other hand, the dependence on field instruments limits the accuracy of the RTTM systems. Thus, measurement errors can potentially trigger leak alarms. Besides the measurement errors, sudden changes in the flows due to transients or slack flows will also create false alarms. Moreover, these systems are sensitive to the fluid properties; thus, they will need to be recalibrated for different patches of fluids or different fluids.

2.3.2.6. *Supervisory Control and Data Acquisition System (SCADA)*

The internal LDSs can be controlled by SCADAs which are computer-based communication system. SCADAs collect the flow-rate, pressure, or temperature from the field infrastructures and process them using internal LDSs' methods. The final decisions are often made by the experienced operators, who are trained to detect leaks' signals from the acquired data. The operators always try to minimize the false alarms, so they often misinterpret the small leaks. To compensate for this issue, pipeline operators use Computers Pipeline Monitoring which are computer systems with algorithms to evaluate the data from field infrastructures. They enhance the judgments of pipeline operators when the interventions or shutdowns phases occur [36]. Pipeline operators can use two of these systems together to improve their leak detection rates.

2.4. Pipelines' protective tapes

To protect pipelines from external corrossions or damages, they are wrapped in the protective tapes. These tapes are often made of Low-Density Polyethylene (LDPE) and had the thicknesses from 0.02" (20 mils) to 0.05" (50 mils). Since there are no regulations for the protective tapes, their constructions vary depend on the

manufacturers. However, the tapes are often constructed of two layers: the adhesive layers, and the protective layers. The adhesive layers can be constructed of synthetic rubber and resins, and the protective layers can be constructed by LDPE. Workers can install the tapes by either hands or machines.



Figure 2.10 – Protective Wrap on Pipeline [56]

In order to be used as a smart membrane, the adhesive layers of protective tapes must be modified to allow stretching.

2.5. Strain Gauge and Wheatstone bridge

Strain gauges have been used as the primary instruments to measure strains. They are constructed of thin metal films glued on polymer substrates. The metal films are folded to reduce the total lengths of the devices. The strain gauges nomenclature are showed in figure 2.11.

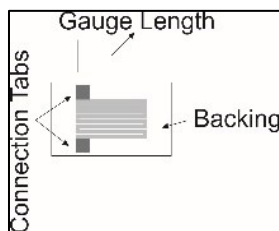


Figure 2.11- Strain gauge nomenclature

The strain gauges are glued on the specimens using specialized glue which provides high adhesion. As the specimens and strain gauges deform, the strain gauges' resistances change. The change in the resistance of the strain gauge is governed by the equation

$$R = \frac{\rho L}{A} \quad (2.1)$$

Where R is the strain gauge resistance (Ω), ρ is the resistivity (Ωin), L is the total length of the strain gauge (in), and A is the cross-section area of the strain gauge (in^2). To measure this change, strain gauges are connected to Wheatstone bridge circuits as their resistors.

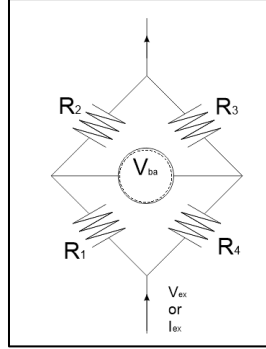


Figure 2.12 - Wheatstone bridge circuit with resistors in the conventional order.

Wheatstone bridge has the ability to measure small changes in resistances of its resistors. If one Wheatstone bridge's resistor is replaced by a strain gauge, it is called Quarter Wheatstone bridge, or Quarter-bridge. If two resistors are replaced by two strain gauges, it is called Half Wheatstone bridge, or Half-bridge. If all resistors are replaced by strain gauges, the circuit is called Full Wheatstone bridge, or Full-bridge. The Wheatstone bridge uses constant voltage as the excitation source. However, the constant current source can be used to reduce the nonlinearity error [37].

As strain gauge is installed on the specimen, it can be approximated as a thin metal film glued on the substrate, i.e. the specimen. By taking logarithm derivative and applying thin film assumption, equation (2.1) becomes

$$\frac{dR_f}{R_f} = \varepsilon_L (1 + \nu_f^2) \left(1 + \nu_s + \frac{\nu_f(1-\nu_s)}{1-\nu_f} \right) \quad (2.2)$$

In which R_f is the resistance of the film. ε_L and ε_w are the longitudinal strain and transverse strain, respectively. ν_f and ν_s are the Poisson ratio of the film and the

substrate, respectively. The equation 2.2 can be used to calculate changes in resistances of any thin films, i.e. strain gauges, using strains from the substrate. The first half of the equation 2.2 represents the substrate's axial strain and transverse strain. The other half is the combination of substrate's and film's Poisson ratio. The equation indicates that the change in film's resistance is dependent on the initial resistance, and Poisson ratios of the film and substrate. If the circuit uses constant current as excitation source, the voltage measured between two arms is

$$V_{ba} = I_{ex} \frac{R_1 R_3 - R_2 R_4}{R_1 + R_2 + R_3 + R_4} \quad (2.3)$$

In this equation, V_{ba} is the voltage between the arms (V), I_{ex} is the current excitation (A), and R is the resistance (Ω).

2.5.1. Quarter-Bridge

In the Wheatstone circuit, if one resistor is replaced with an active strain gauge, then the circuit is called Quarter-bridge. For constant excitation current, the strain can be calculated using

$$\varepsilon = -4 * \frac{V_{ba}}{GF*(V_{ba} + I_{ex}R)} \quad (2.4)$$

Where ε and GF are the strain and the gauge factor, respectively. Comparing to the other Wheatstone bridge configurations, Quarter-bridge has the lowest sensitivity because its voltage change is created by one strain gauge. This bridge is also subjected to the highest nonlinearity error for large strain applications [38] [39]. Moreover, temperature change will cause thermal expansion in the strain gauge and affect the voltage output [40]. Despite of the disadvantages, Quarter-bridge is simple and compact to use. In addition, the offset voltage, or voltage at zero deformation, in Quarter-bridge can be easily reduced by using potentiometers.

2.5.2. Half-Bridge

When two strain gauges are used to replace two resistances in Wheatstone bridge, they form Half-bridge circuit. This configuration is twice as sensitive as the Quarter-bridge [41]. The nonlinear error is also smaller than the Quarter-bridge [42]. Since two strain gauges can be chosen in different orders, there are different

equations to calculate the strains from Half-bridge. In this research, strain gauges R_1 and R_3 are selected and positioned perpendicular to the other, therefore, the equation to calculate the strain is

$$\varepsilon = -\frac{4V_{ba}}{GF(1-\nu_s)(V_{ba}-I_{ex}R)} \quad (2.5)$$

Note that ν_s in this equation is the Poisson ratio of the specimen. This configuration does not compensate for the temperature change. This problem can be fixed by replacing resistances R_2 and R_4 with two dummy strain gauges. Dummy strain gauges are strain gauges that are exposed to the similar temperatures as the active strain gauges but not to the strains.

2.5.3. Full-Bridge

The highest sensitivity can be archived by using four active strain gauges to replace all resistors [41]. This configuration provides the highest sensitivity when strain gauges are positioned appropriately. For instance, when strain gauges R_1 and R_3 are installed on the upper surface of the bending specimen and R_2 and R_4 are installed on the lower surface, the bridge will give the highest sensitivity during bending because two strain gauges undergo tensions and the others undergo compressions. However, this setup is not appropriate for the tensile specimen as all strain gauges are equally elongated, and there will be no voltage output. In order to measure tensile strain using the Full-bridge, strain gauges R_2 and R_4 should act as Poisson gauges, which measure the strains due to the Poisson effects. As a result, the general rules for using Full-bridge is to avoid same deformations on all four strain gauges.

2.6. Conductive ink and Resistive ink

Two candidate inks that are used in this study are the conductive ink, i.e. silver ink, and the resistive ink, i.e. carbon ink, both of them are supplied by **Methode** Inc. Conductive ink has higher conductivity and adhesion than resistive ink, thus, it is the first choice for applications requires high conductivities [43].

The resistive ink has lower conductivity than the conductive ink and has been used in various commercial products such as membrane switches and printed circuits. The main advantage of resistive ink is that it is inert over time and chemically

resistant [44]. Resistive ink is also cost effective comparing to conductive ink, however, it has a tendency to precipitate and to form wax-like substance. This tendency is hazardous if the resistive ink is left inside the printer because it will clog the print head. Thus, the resistive ink should be completely removed from the printer after the experiments.

The main advantage of both inks used in this study is that they do not require UV light to cure, thus, they simplify the manufacturing process and decrease the uncertainty between different batches. On the other hand, both conductive and resistive inks show the decrease in resistance after printing. This decrease is observed to be rapid at first but slowed down after 1 hour and completely stop after 24 hours. As a result, the printed sensors should be left to dry at room temperature for 24 hours before the experiments or measurements. The material properties of these inks are showed in the table below

Table 2-2: Comparison between Conductive 9101 Ink and Resistive 3804 Ink.

	Silver 9101 (Conductive) Ink	Carbon 3804(Resistive) Ink
Viscosity	3.5 cps	6 cps
Density	1.2 g/ml	1.0 g/ml
Surface Tension	55 dynes/cm	26 dynes/cm
Print Thickness	1-10 micron	1-10 micron
Min. Line Width	75 micron	75 micron
Electrical Resistance	25 milliohm per square	3000 Ohm per square
Color	Metallic Gold	Black

Notice that the printed thicknesses are expected to vary because of the low-cost print head. This uncertainty is the major drawback of using the low-cost printer to print electronic devices.

2.7. Summary

There are various LDSs available to detect different leaks' sizes. Most of these systems are optimized so that they minimize false alarms, and therefore they often overlook the pinhole leaks. Internal LDSs can be incorporated into existing pipelines, however, their accuracies are limited to the accuracies of field infrastructures which give them the data. Most of these infrastructures do not have

the accuracy to distinct small leaks from environmental noises. Thus, internal LDSs are generally blind to the pinhole leak. On the other hand, external LDSs have high accuracies and potential to detect pinhole leaks. They require their own sensors that are installed along the pipes. Thus, they are expensive, and they require complex installation procedures. Afzal summarized these advantages and disadvantages of those systems in the table below

Table 2-3: Summary of LDS methods available and their abilities to detect pinhole leaks.

External Methods		Pinhole Leak Detection
Visual Leak Detection [12]		
<u>Advantages</u>	<u>Limitations</u>	
Requires no tools or equipment	Up to three-week detection time	Only if the damages become observable on the site.
Location of leak is immediately known in most cases	Small leaks may not be readily apparent at ground level	
Can be used in hard to reach location like mountain and wetland	Dependent on the diligence of personnel inspecting the ROW	
	Expensive for continuous monitoring	
Acoustic Emissions [45]		Pinhole Leak Detection
<u>Advantages</u>	<u>Limitations</u>	
Automatic and continuous method	Environmental noise reduces the sensibility	Not capable.
Accuracy and Reliability	Sensors are high cost	
Leak size estimation		
Robust		
Can be incorporated into existing pipeline		
Fiber Optic Cables [12]		Pinhole Leak Detection
<u>Advantages</u>	<u>Limitations</u>	
Automatic and continuous method	Difficult to be incorporated into existing pipelines.	Capable if the pinhole leaks occur at the cables' locations.
Localizing leaks	Multiphase flow is problematic	
Leak size estimation	High cost	
Immune to electromagnetic interference	Low redundancy	
Reasonable response time		
High sensitivity		
Vapor Sensing Tube [45]		Pinhole Leak Detection
<u>Advantages</u>	<u>Limitations</u>	
Automatic and continuous method	Slow response time	Capable if the pinhole leaks occur at the tubes' locations for a period of time.
Localizing leaks	Only used for short pipe	
Leak size estimation	High cost	
Immune to different fluid types		
Liquid Sensing Cables [12]		

<u>Advantages</u>	<u>Limitations</u>	Pinhole Leak Detection
Automatic and continuous method	Cannot estimate leak size	Capable if the pinhole leaks occur at the cables' locations for a period of time.
Good response time	Difficult to be incorporated into existing pipelines.	
Work for underground pipeline	Multiphase flow is problematic	
Immune to different fluid types	Not a robust system because the cable needs to be replaced before coming back to service	
Response time is in seconds to minutes	High cost	

Internal Systems		Pinhole Leak Detection
Pipeline Inspection Gauge (PIG) [46]		
<u>Advantages</u>	<u>Limitations</u>	
High accuracy and sensitive for leak location	Require launch/receive stations. Pipelines must have constant diameters.	Capable with the experience operators. This technique generates a large amount of data that require months to be analyzed.
Leak localization	Not continuous systems. Data require time to be analyzed.	
Simple, can be used on existing pipelines	May have problems with small and complex pipeline	
Volume Balance Methods [45]		Pinhole Leak Detection
<u>Advantages</u>	<u>Limitations</u>	
Can be incorporated into existing pipelines	May generate false alarms in transient stages	Not capable in a short time. This method only detects pinhole leak after a significant loss of product.
Low maintenance	Long response time for pinhole leak	
Low costs	Leak localization is not possible	
Can detect leaks that are less than 5% in minutes to hours	Generate frequent false alarms if thresholds are small	
Pressure Monitoring [12]		Pinhole Leak Detection
<u>Advantages</u>	<u>Limitations</u>	
Can be used in transient stages	Small leaks, existing leaks, and leaks during slack line conditions cannot be detected	Not capable.
Localization leak is possible	May generate false alarms in transient stages	

Leak size estimation is possible		
Can be incorporated into existing pipelines		
Low maintenance		
Low costs		
Can detect leaks that are 5% in minutes		
Statistical Analysis [11] [12]		Pinhole Leak Detection
<u>Advantages</u>	<u>Limitations</u>	
Can detect leak during transient stages	Small leaks, existing leaks, and leaks during slack line conditions cannot be detected	
Less false alarms with large data	Not accurate in leak size estimation	
Localization leak is possible	Depend on field instruments' qualities	
Can be incorporated into existing pipelines	Require large data to make decision	
Robust Sensors can be located far from the others	Cannot (normally) distinguish between multiple leaks on one pipeline	
RTTM [11] [12]		Pinhole Leak Detection
<u>Advantages</u>	<u>Limitations</u>	
Localization leak is possible	Existing leaks cannot be detected	
Leak size estimation is possible	Difficult to train operators to use	
Immune to transient stages	Must be customized for each pipeline systems	
Cost effective	Difficult in maintenance	
Sensors can be located far from the others	Depend on field instruments' qualities	
Can be used to predict conditions in the pipeline, such as tracking PIGs, tracking liquids' phases.	High alarm rates in the transient stage.	
	Sensitive to fluid properties.	
	Require large number of parameters Require experts to operate and maintain.	

Besides the developments of LDSs, printed electronics also develop and introduce new technologies, such as conductive and resistive inks. These inks had been formulated before. However, they are recently more printer friendly, and they can be used in various low-cost printers. Recent researches indicated that printed strain gauges are more sensitive than their regular counterparts [44]. Even though most of the strain gauges in those researchs were printed using specialized printers, some studies demonstrated that low-cost inkjet printers can be used [47].

The above studies and technologies suggest that external LDSs with the printed sensors will create a system which is high accurate, robust, and inexpensive. As a result, the smart membrane has the potential to be used together with other systems or even replace them.

2.8. References

- [1] CEPA, *Liquids Pipeline* [Online]. Available: <http://www.cepa.com/about-pipelines/types-of-pipelines/liquids-pipelines>. [Accessed 31 March 2016].
- [2] Alyeska Pipeline Service Company, *Pipeline Facts* [Online]. Available: <http://www.alyeska-pipe.com/TAPS/PipelineFacts>. [Accessed 02 April 2016].
- [3] L. Song. (2012). *Few Oil Pipeline Spills Detected by Much-Touted Technology* [Online]. Available: <http://insideclimatenews.org/news/20120919/few-oil-pipeline-spills-detected-much-touted-technology>. [Accessed 30 June 2015].
- [4] C. Cheng, "Evaluation of Pipeline Leak Detection Technologies," M.Eng. thesis. Dept. Mech. Eng., University of Alberta, Edmonton, 2013.
- [5] International Association of Oil & Gas Producers, "Risk Assessment Data Directory- Summary". OGP, 2010.
- [6] Committee on the Safety of Marine Pipelines et al., "Maintaining the Integrity of the Marine Pipeline Network," in *Improving the Safety of Marine Pipelines*. Washington, D.C., National Academy Press, 1994, pp. 45.
- [7] A. Swift. 2011. *The Keystone XL Tar Sands Pipeline Leak Detection System Would Have Likely Missed the 63,000 Gallon Norman Wells Pipeline Spill* [Online]. Available: <https://www.nrdc.org/experts/anthony-swift/keystone-xl-tar-sands-pipeline-leak-detection-system-would-have-likely-missed>
- [8] D. Shaw et al., "Leak Detection Study - DTPH56-11-D-000001," U.S. Department of Transportation Pipeline and Hazardous Materials Safety Administration, Worthington, 2012.
- [9] D. Mawhinney. (2015). *Corrosion Pit* [Online]. Available: https://en.wikipedia.org/wiki/Pitting_corrosion#/media/File:Corrosion.Pit.jpg.

- [10] Alaska Department of Environmental Conservation, "Technical Review of Leak Detection Technologies," Alaska Department of Environmental Conservation.
- [11] J. Zhang et al., "Review of Pipeline Leak Detection Technologies," Pipeline Simulation Interest Group, Prague, 2013.
- [12] J. Summa, "Pipeline Leak Detection Operational Improvements: An Overview of Currently Available Leak Detection Technologies & US Regulations/Standards," in *6th Pipeline Technology Conference*, Hannover, 2011.
- [13] G. Geiger, "State-of-the-Art in Leak Detection and Localization," in *Pipeline Technology 2006 Conference*, Germany, 2006.
- [14] P. Siebenaler et al., *Detection of Small Leaks in Liquid Pipelines: Gap Study of Available Methods (PL-1)*, Southwest Research Institute, 2007.
- [15] J. C. Liou, and L. Cui, T. Li, "Hazardous Liquid Leak Detection Techniques and Processes," General Physics Corp., 2003.
- [16] Integrity Diagnostics, "Introduction to Acoustic Emission [Online]. Available: http://www.idinspections.com/?page_id=126. [Accessed 26 May 2013].
- [17] R. K. Miller et al., *A Reference Standard for the Development of Acoustic Emission Pipeline Leak Detection Techniques*, NDR&E International, pp. 32, 1999.
- [18] Y. Gao, "A Model of the Correlation Function of Leak Noise in Buried Plastic Pipes." *Journal of Sound and Vibration*, pp. 133-148, 2004.
- [19] J. Zhang, "Statistical Pipeline Leak Detection for All Operating Conditions," *Pipeline & Gas Journal*, vol. 2, pp. 42-45, 2001.

- [20] G. Hessel, "A Neural-network Approach for Acoustic Leak Monitoring in Pressurized Plants with Complicated Topologies," *Control Engineering Practice*, vol. 4, no. 9, pp. 1271-1276, 1996.
- [21] H. Dasilva, et al., "Leak Detection in Petroleum Pipelines Using a Fuzzy System," *Journal of Petroleum Science and Engineering*, vol. 49, no. 3-4, pp. 223-238, 2005.
- [22] P. Lee et al., "Leak Location Using the Pattern of the Frequency Response Diagram in Pipelines: A Numerical Study," *Journal of Sound and Vibration*, pp. 1051-1073, 2005.
- [23] J. Hu, et al., "Detection of Small Leakage from Long Transportation Pipeline with Complex Noise," *Journal of Loss Prevention in the Process Industries*, vol. 24, pp. 449-457, 2011.
- [24] E. Rochatm, and M. Nikles, "Fiber Optic Asset Integrity Monitoring Using Brillouin-Based Distributed Sensing for the Oil and Gas and Energy Industry: Challenges and Achievements," in *Proceedings of the 22nd International Conference on Optical Fiber Sensors*, 2012.
- [25] D. Inaudi, R. et al., "Detection and Localization of Micro-Leakages using Distributed Fiver Optic Sensing," in *7th International Pipeline Conference*, 2008.
- [26] D. Inaudi, and B. Glisic, "Long-Range Pipeline Monitoring by Distributed Fiber Optic Sensing," *Journal of Pressure Vessel Technology*, vol. 132, 2010.
- [27] Process Online, *Digital Pipeline Leak Detection* [Online]. Available: <http://www.processonline.com.au/articles/29927-Digital-pipeline-leak-detection-using-fibre-optic-distributed-temperature-sensing>. [Accessed 26 June 2013].
- [28] C. Apps et al., "Evaluation of Distributed Leak Detection Technologies for Liquid Pipeline," in *C-Fer Technologies*, Edmonton, 2012.

- [29] S. Chet et al., "The Application of a Continuous Leak Detection System to Pipelines and Associated Equipment," *IEEE*, pp. 900-906, 1989.
- [30] D. Atherton, and L. Clapham, *In-Line Inspection Tools for Pipelines* [Online]. Available: <http://www.physics.queensu.ca/~amg/expertise/inline.html>. [Accessed 03 April 2016].
- [31] M. Beller, "Pipeline Inspection Utilizing Ultrasound Technology on the Issue of Resolution," *Pigging Products and Services Association*, 2007.
- [32] H. R., "Smart Pigging Philosophy," in *The NACE International Annual Conference and Exposition*, Concord, 1996.
- [33] T. Chris, "Pipeline Leak Detection Techniques," *Annual Computer Science Series*, 2007.
- [34] A. Afifi et al., "Pressure Point Analysis for Early Detection System," *IEEE*, 2011.
- [35] Krohne Inc., *PipePatrol-Pipeline Leak Detection* [Online]. Available: <http://krohne.com/en/products/systems/pipepatrol/>
- [36] API, "Computational Pipeline Monitoring for Liquid Pipelines: Pipeline Segment," *American Petroleum Institute*, 2007.
- [37] C. Silva, *Vibration Monitoring, Testing, and Instrumentation*, Canada: CRC Press, 2007.
- [38] Measurements Group, "Wheatstone Bridge Nonlinearity," Measurement Group, 2000.
- [39] Micro-Measurements, "Errors Due to Wheatstone Bridge Nonlinearity," Micro-Measurements, 2010.
- [40] Micro-Measurements, "Strain Gage Thermal Output and Gauge Factor Variation with Temperature," Micro-Measurements, 2014.
- [41] K. Hoffmann, "Applying the Wheatstone Bridge Circuit," HBM.

- [42] Vishay Precision, "Errors Due to Wheatstone Bridge Nonlinearity," Vishay Precision Group.
- [43] N. D. Sankir, "Flexible Electronics: Materials and Device Fabrication," Ph.D. dissertation. Mat. Sc. Eng., Virginia Polytechnic Institute and State Univ., Blacksburg, VA, 2005.
- [44] S. S. Bhore, "Formulation and Evaluation of Resistive Inks for Applications in Printed Electronics," M.S. thesis, Dept. Chem. and Paper Eng., Western Michigan Univ., Michigan, 2013.
- [45] The U.S. Department of Transportation, "Leak Detection Technology Study," The U.S. Department of Transportation, 2007.
- [46] PTC, "Reliable and Cost Effective Leak Detection with a New Generation of Ultrasonic PIGs," in *7th Pipeline Technology Conference 2012*, 2012.
- [47] B. Andò, "All-Inkjet Printed Strain Sensors," *IEEE*, vol. 13, no. 12, pp. 4874-4879, 2013.
- [48] ICF International, "North American Midstream Infrastructure through 2035: Capitalizing on Our Energy Abundance". INGAA Foundation, Washington, D.C., 2014.
- [49] AOPL and API. *Pipeline 101* [Online]. Available: <http://www.pipeline101.org>.
- [50] G.A.O., "Pipeline Safety, "U.S. Govt. Accountability Office: Collecting Data and Sharing Information on Federally Unregulated Gathering Pipelines Could Help Enhance Safety, Washington, D.C.,2012.
- [51] Argonne National Laboratory, "Natural Gas Pipeline Technology Overview," U.S. Dept. of Energy, Oak Ridge, TN, 2007.
- [52] INGAA, "Interstate Natural Gas Pipeline Desk Reference," INGAA, 2009.
- [53] P. W. Parfomak, "Keeping America's Pipelines Safe and Secure: Key Issues for Congress," Congressional Research Service, 2013.

- [54] INGAA Foundation, “Building Interstate Natural Gas Transmission Pipelines: A Primer,” INGAA, 2013.
- [55] T. E. Bell. (2015). *Pipelines Safety and Security: Is It No More Than a pipe Deam?* [Online]. Available:
<http://www.tbp.org/pubs/Features/W15Bell.pdf>.
- [56] Azh7. *The World's Longest Ammonia Pipeline from Russia to Ukraine*. [Online]. Available:
https://en.wikipedia.org/wiki/Pipeline_transport#/media/File:Ammiakoprovod_NS.jpg
- [57] Bryan, *Close Up Pictures of Gas Line Explosion Damage Taken from the Intersection of Glenview Dr. & Earl Ave., Facing South on Glenview Dr., in San Bruno, CA*. [Online]. Available:
https://en.wikipedia.org/wiki/2010_San_Bruno_pipeline_explosion#/media/File:Pipe-from-Sanbruno-explosion.jpg

Chapter 3: Design of the Smart Membrane

3.1. Design Philosophy

The smart membrane was expected to have more advantages than the other LDSs. It should inherit the accuracies of the external systems while keeping the cost low. This goal was achieved by using the appropriate sensors and sensor's density on the membrane. The sensors in this study referred to Wheatstone bridge circuits which were made of printed strain gauges. The PSGs were inexpensive and more sensitive than the current strain gauges. The wireless system, which sends a signal to the data acquisition system, was out of the scope of this study. This study focused on creating a working prototype of the membrane and an optimized design for the smart membranes.

The designs were based on the existing protective wrapping technologies in pipelines; thus, the membranes' thicknesses were varied from 0.03" to 0.05" (30 mils to 50 mils). The study would indicate the appropriated lengths for each thickness in this range. The membrane's material was Low-Density Polyethylene (LDPE) which was similar to the protective wrap's material. In order for the wireless receivers to receive the sensor's signals, the signals must have S/N of 30 dB under applying forces. There were two designs proposed in this study. The first design aimed to pinpoint the leak location using signals from various sensors. It would be optimized to detect the pressure that was calculated by pipe's inner pressure and leak's diameter. The second design focused on using one sensor to detect the presence of the leak substances. Thus, it sacrificed the leak localizing ability for the cost effectivity. The second design was optimized to detect the presence of 1 lb leak substances. Due to the high internal flow-rate of the pipe, it would take less than 1 second for 1 lb leak substance to accumulate in the second design.

Before printing the sensors, a study on membrane stresses and strains were carried out. In this study, all the possible loading situations on the membrane were evaluated. After that, the inks and printer were studied to evaluate their properties.

Then, the strain gauges were printed and tested in the four points bending test. Finally, a prototype of the membrane and its simulation model were built. The prototype went through the dimple test, and its sensor's voltage outputs were compared to the simulation model's outputs.

3.2. Designs of smart membrane

- The proposed designs

The initial membrane was designed with multiple sensors installed on its surface. This membrane was wrapped around the entire pipeline segment which had the length of 39' and diameter of 36". As pinhole leak occurred, it applied small pressure on the membrane. Multiple sensors were used to localize this pressure by interpolating their voltages' magnitudes. The second design involved wrapping multiple small membranes around a pipe segment. Each membrane had one main sensor and one back up sensor facing the ground. The sensor was printed at the membrane's center to detect the strain at both ends. The ends of the membrane would be taped to the pipe. The taped ends helped to capture the leaked products that, subsequently, imposed a strain on the membrane.

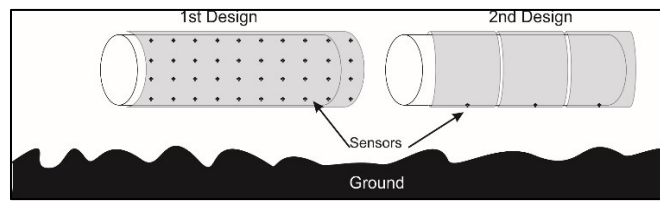


Figure 3.1 - Two designs of the membrane. The 1st design localizes the leak by interpolating voltages from multiple sensors. The 2nd design detects the presence of the leak at the bottom of the membrane.

- Strain distribution study

The design of the membrane began with the study of the strain distribution during loadings. First, 36" pipe with a length of 39' was modeled in ANSYS APDL. It was wrapped around by the membrane with the same geometry. In order to reduce calculation time, the shell element Shell281 was used to model both pipe and membrane. The contacts between the pipe and the membrane were modeled as Surface-to-Surface contact with element Conta174 and Targe170. Since the

membrane was softer than the pipe, it was used as contact element, and the pipe will be used as target element. By ANSYS's definition, contact elements could not penetrate the targets. However, target elements could penetrate the contact surfaces [1]. To simplify the simulation, the dynamic friction coefficient between rubber and steel with the value of 0.5 was used. This coefficient was reasonable because it represented a slow movement between rubber and steel [2]. Both the ends of the pipe and the membrane were fixed to simulate the real boundary conditions.

This model was used to study the weakest region on the membrane, i.e. where the leak caused minimal strain. The leak's pressure was derived from the pipe's pressure of 600 psi and the leak's diameter of 0.157". The leak force was calculated to be 11.6 lbf, and it was applied as a point force on the membrane. This force was only used for reference, the results for the other forces were similar. For every force's location along the pipe, the hoop strains at the opposite side were collected. The force was applied at the middle of the membrane first, then it was moved to the end of the membrane. The highest hoop strain was plotted against the leak's location as it moved across the membrane.

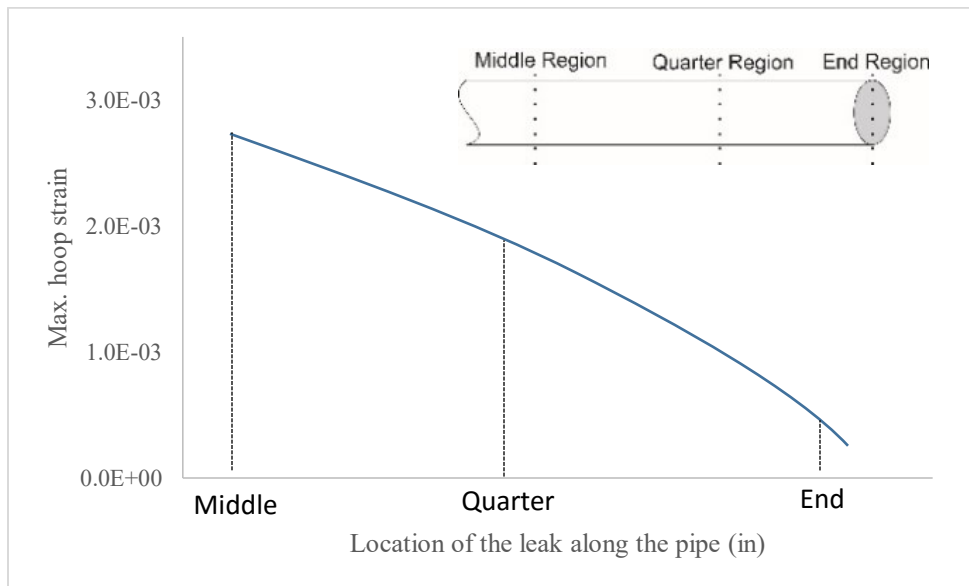


Figure 3.2 - Maximum hoop strain caused by the leak as it moved from the pipe's middle region to end region. This fact indicated that the sensor density of the 1st design must be varied along the pipe to account for the strain difference.

The leak occurred at the membrane's end caused minimal strain in the membrane. This was because this region has highest constraints on the membrane. On the other hand, the leak occurred at the pipe's center caused the highest strain in the membrane.

The first design's goal was to detect outward pressure at the leak locations. The design aimed to pinpoint the leak's location by interpolating the voltages from sensors surrounding the leak. In order to achieve this goal, multiple sensors were printed on the membrane. From the previous study, the sensor densities would be different along the pipe because the strain distributions were different. The highest sensor densities occurred at the ends of the membrane because of the low strains. The sensor densities reduced away from the ends and reached a minimum at the center of the pipe. Thus, different pipelines' lengths required different membrane designs. This fact complicated the data acquisition systems and increased the system's cost. In addition, this design was not universal. If rupture broke the membrane, the entire pipe segment would need a new membrane which was specially designed for it. As a result, this design was not economically sound even though it could localize the leak precisely.

The second design was created to compensate these disadvantages. It aimed to use the minimum amount of sensors on the membrane. Also, the membrane should be universal so that it could be wrapped around any pipes with the same radius. As a result, the membrane was designed to detect the weight of the leaked products. It consisted of one primary sensor and one backup sensor located on the membrane's bottom, and these sensors would face the ground. As the leak occurred, the leaked products accumulated and stretched the membrane's lower surface. By using the above model with the force of 1 lbf distributed on the bottom of the pipe, the simulation showed that hoop strains along the membrane bottom were higher than axial strains. Thus, the strain gauges in the sensor should be positioned along the circumference to measure the hoop strain.

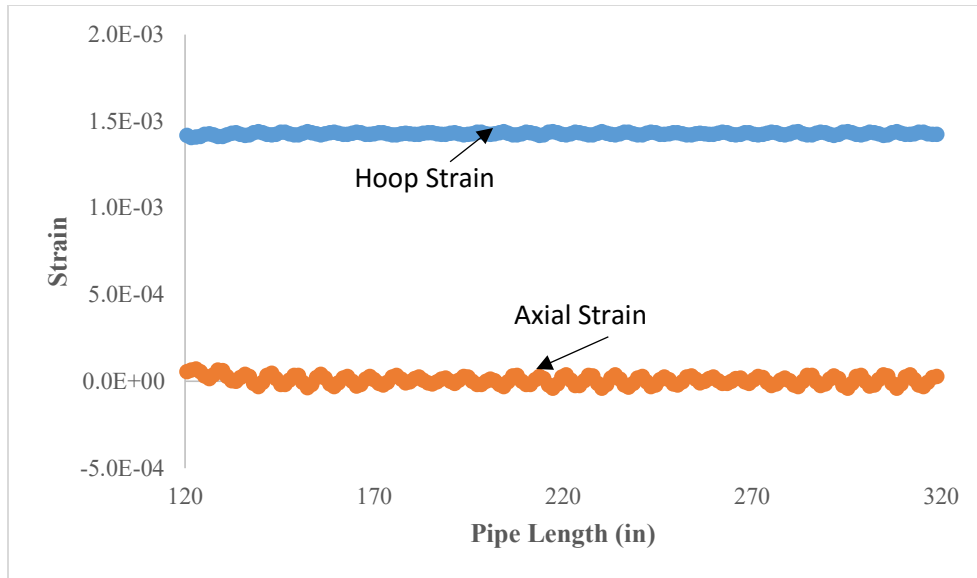


Figure 3.3 - Hoop strain and axial strain distributed along the membrane under 1 lb of leak substance. This fact indicated that the 2nd design should measure the hoop strain for the highest signal.

The advantages of this design were that they could detect any leaks with different sizes. Even the smallest leaks and creep could be detected given enough time for leaked products to accumulate. Moreover, the membrane could be reused if the leaked amount was small. If rupture broke the membrane, that broken segment could be replaced quickly while other segments were not affected. The membranes could also be employed on pipelines that had multiphase fluids, and they would not be affected by the transient phases of the pipelines. Thus, this design would be chosen for the smart membrane.

- Membrane installation methods

The smart membrane was expected to be installed on the pipeline using the similar techniques as the protective wraps. However, the membrane would not be glued to the pipes to allow it to deform. Two installation methods were suggested in this study. The first method should be used for new pipelines in which the pipes' segments had not been connected. This method involved a long membrane that covered the entire pipe's segment. The membrane was divided into smaller segments using stainless steel wires to replicate the taped ends.

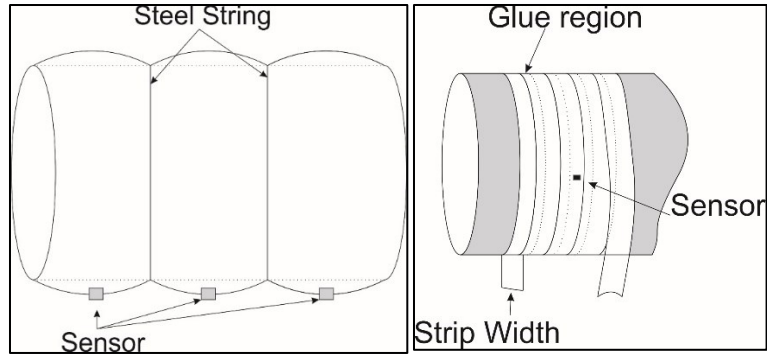


Figure 3.4 - Two methods for installing the smart membrane on the pipe.

The other design was to manufacture the membrane as a long tape with glue on one edge. As the tape was wrapped around the pipe, the glue side overlapped the outer surface of the previous layer; thus, it formed a segment. This design was used for the existing pipelines in which the first method could not be used.

3.3. Design of Sensors

As mentioned in chapter 2, the Wheatstone bridge could be connected in several ways to create different configurations. Each configuration was designed to detect strain in a specific scenario. In order to choose the appropriate configuration for the smart membrane, it was necessary to consider the strain states that the sensor would experience on the membrane.

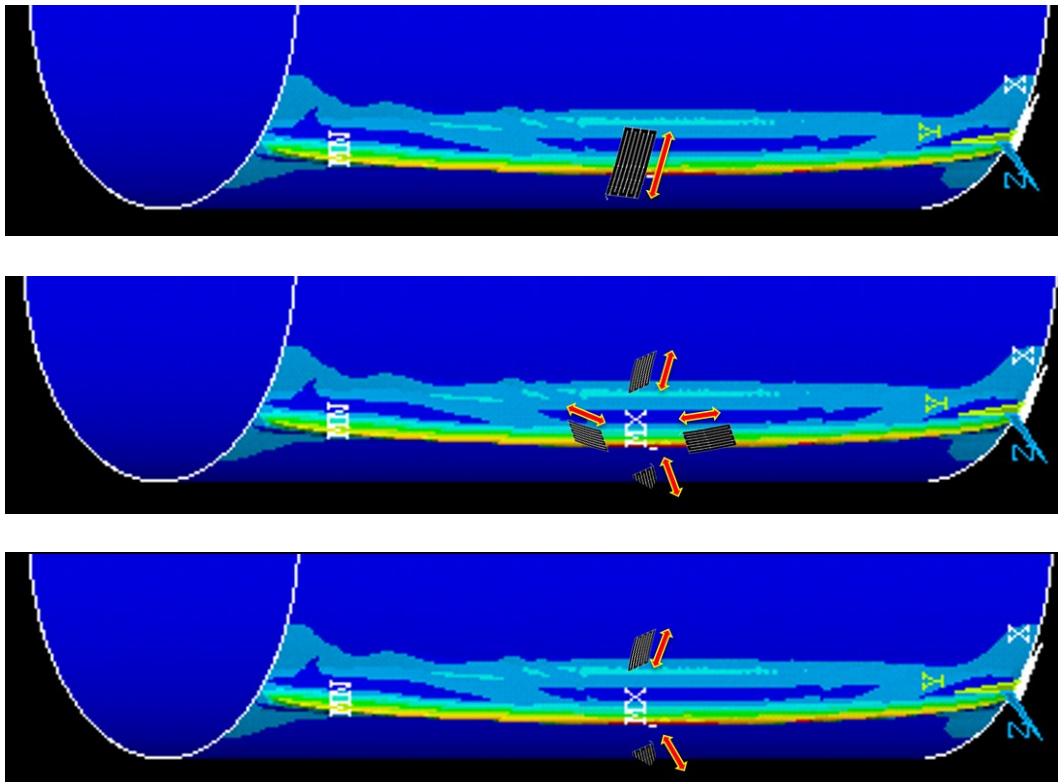


Figure 3.5 - Different Wheatstone bridge installed on the membrane. (Top) Quarter-bridge – Small voltage output, (Middle) Full-bridge – Small voltage output as all sensors experienced tensions, (Bottom) Half-bridge – Highest voltage output.

As indicate in figure 3.5, the Quarter-bridge could detect the hoop strain. However, this signal would be weak because it was caused by the deformation of one strain gauge. The Full-bridge configuration generated the highest signal when one pair of strain gauges undergo tension and the other undergo compression. Since there was only tension in the membrane, the signal from the Full-bridge was reduced predicted by equation 2.3. On the other hand, Half-bridge created the highest signal as stretched strain gauges amplifying the signal from others. Based on the analysis above, the Half-bridge using R_1 and R_3 was chosen because it gave highest. The strain gauges should be positioned so that both of them went through similar elongations. Thus, they should be positioned along the circumference where the highest strain occurs.

3.3.1. Printed strain gauge design

Before designing the strain gauge, an ink study had to be carried out to determine the properties of the inks and the capacity of the printer. The sensors in this study were printed on a Polyethylene Terephthalate (PET) paper supplied from **Methode Inc.** using the Inkjet printer **EPSON 4900**. The PET papers were designed by **Methode** to work with their conductive and resistive inks. The printer was a low-cost inkjet that could print on large format paper. The conductive and resistive inks were filled into the refillable cyan and yellow cartridges, respectively. Since the resistive inks dried quickly under room temperature, the nozzles must be thoroughly cleaned before printing, and the resistive ink must be taken out after printing. The conductive ink was made of silver, and it had the sheet resistance of $25 \text{ m}\Omega$ per squared (depending on the drop size). The other one was the resistive ink, which was made of carbon and had a sheet resistance of $5,000 \text{ }\Omega$ per square. Both of the inks were supplied by **Methode Inc.** Notice that the resistive ink dried quickly and precipitated inside the ink cartridge. Thus, only a small amount of ink was stored at a time, and it would not be used to study the printer's capacity.

To study the printer, two studies were prepared. The first study involved printing out multiple strips using conductive ink with different lengths in the horizontal direction. The sample for this study was showed in figure 3.6

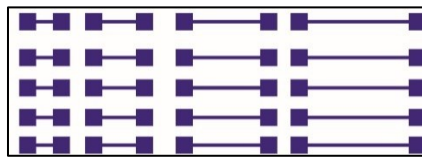


Figure 3.6 - Sample to study the printer's capacity to print long strip. The strips' thickness was 0.039" and their lengths were increased from 0.197" to 1.18".

The thickness of the strip was 0.039" and the length was increased from 0.197" to 1.18". The resistance of each strip was measured using the Fluke 189 multimeter.



Figure 3.7 - Multimeter used in the experiment.

For each specific length, the measurements were repeated five times on five different strips with the same dimensions. The results of the measurement are showed below.

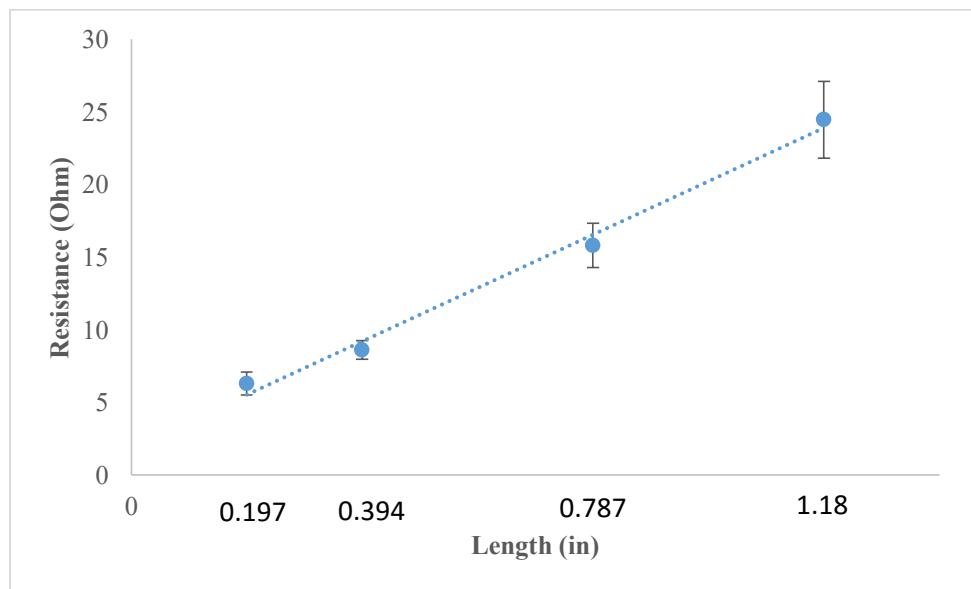


Figure 3.8 - The resistance changed as the length increased. Notice that the error was also increased with the length. Thus, the printer was not able to print long strips.

Note that the error bars were constructed using the standard deviations. From the data, the resistances of the strips increased as the lengths increased and followed the equation 2.1. Note that as the length increased, the error bars also increased. This fact meant that the printer was not capable of consistently printing long strips. Therefore, short strips would be preferred.

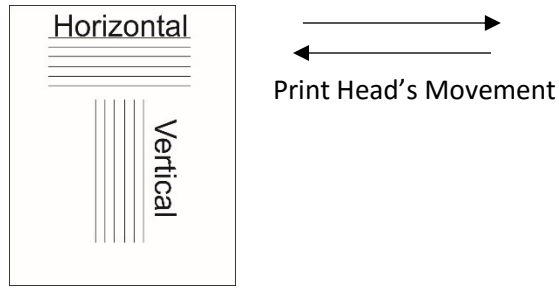


Figure 3.9 - Printing direction according to the printing mechanism.

The second study involved changing the widths of the lines while keeping the lengths constant. In this study, the samples were printed using conductive ink in both horizontal and vertical directions. The idea was to study how the print's directions affect the results. The picture of the actual sample is showed below

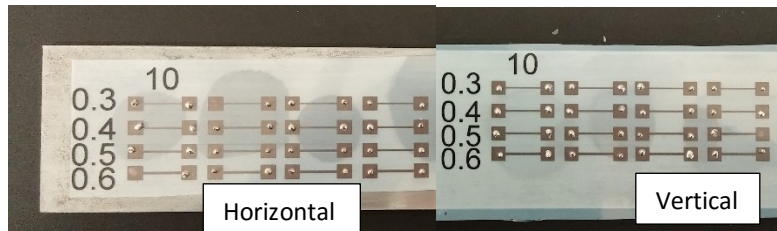


Figure 3.10 – Testing the consistency of strips' thicknesses and the printing directions. Vertical strips (right) are more resistant than horizontal strips (left).

The samples were glued on a steel specimen to prevent it from bending which would change the strips' resistances. The widths of the strips were increased from 0.016" to 0.024" and the lengths were 0.394". Each strip's configuration was measured four times on four different strips for statistical purpose. The result of this study is showed below

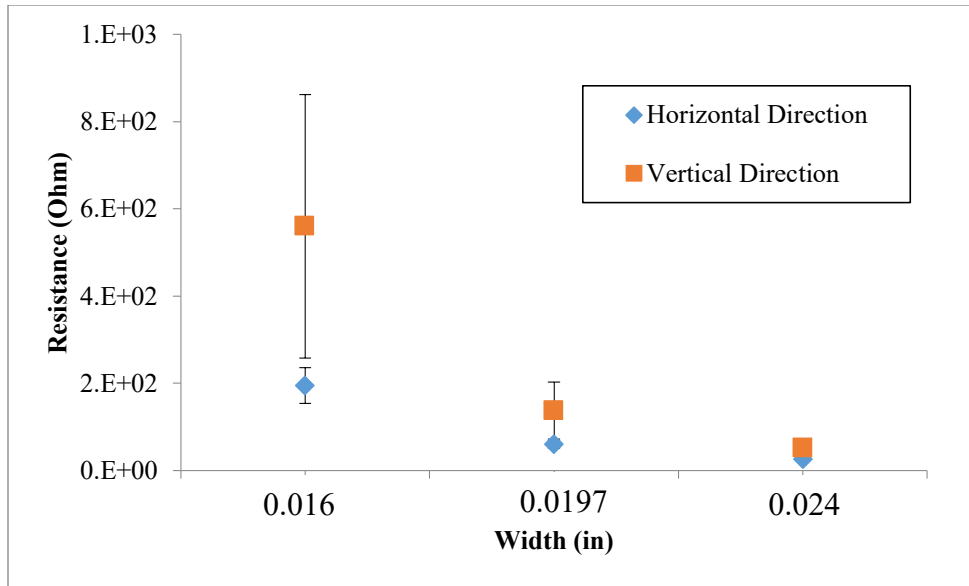


Figure 3.11 - Resistances of the strips printed in horizontal and vertical direction. The uncertainties and resistances of vertical strips were higher than horizontal strips’.

The result indicated that the smaller the width, the higher the resistance as equation 2.1 predicted. As the widths were reduced below 0.0157”, the errors were dominant, and the average resistance was unreliable; thus its result was not showed. The printed directions were also a factor affecting the resistances. As the strain gauges were printed vertically, the resistances were three times higher than their counterparts. The reason for this phenomenal was the printer’s printing mechanism. The vertical strips were constructed by many small horizontal segments laid down by the printhead as it moved across the paper horizontally. Due to the tolerance of the print-head, the “gaps” between those segments were thinner than the overall thickness; thus, they acted as resistors connected in series and raise the resistance of the strip.

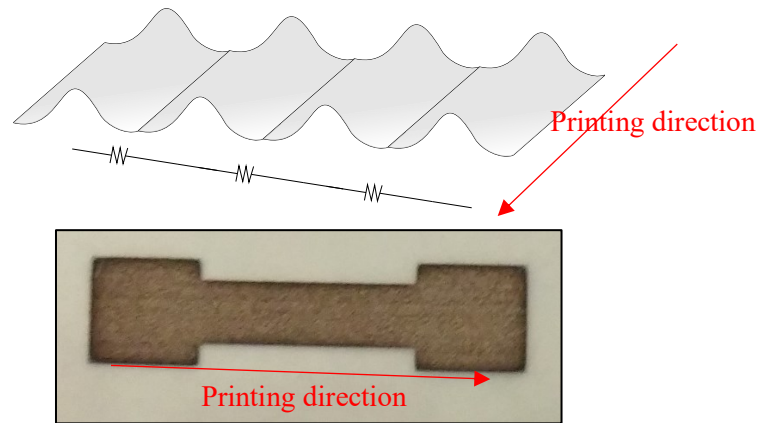


Figure 3.12 - (Top) the gaps between the small segments laid down by the printer acted like the resistances in series. (Bottom) close up of the defected strip that was printed horizontally. Horizontal lines with different thickness (dark/light color lines) could be observed.

In addition, the results indicated that the strip's widths did not vary linearly with the resistances as the equation 2.1 predicted. This problem was expected to come from the fact that strip's thickness decreased as its width decreased.

Based on the results from the two studies, the strain gauge was printed horizontally with the width of 0.0236" and the total length of 3.15". This configuration would give the PSGs consistent resistances and also compatible sizes as the RSGs. Based on the sheet resistance, the resistance of conductive PSG was approximately 3.33 Ω . Note that the conductive printed strain gauge would be preferred as conductive PSG, and the resistive printed strain gauge would be preferred as resistive PSG. The actual picture of the printed strain gauge was showed below

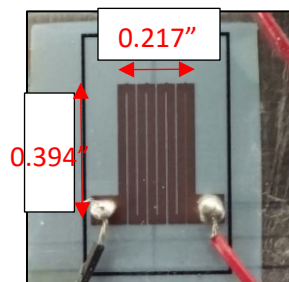


Figure 3.13 - Conductive PSG installed on the steel specimen.

The resistance of the strain gauge was measured using the multimeter, and it had the value of 240.66 Ω . The difference in the resistance indicates that the conductive

ink property was change due to the high temperature in the printer. Based on the sheet resistance of the resistive ink, the resistive strain gauges were expected to have the resistances of 0.4 M Ω . However, the resistive strain gauges, printed in the horizontal direction, had the resistances of approximately 17 M Ω . This difference in resistance could have the same causes as the conductive ink. Thus, specialize printer is recommended for this printing purpose. In addition, the resistance of resistive ink was expected to have higher uncertainty than the conductive ink because the carbon platelet could not be printed with constant thickness [3].

Since the PET paper's limited temperature was 130°C which was lower than the solder's temperature, 300°C, the solder pastes **SolderPlus** had to be used to connect the wires.

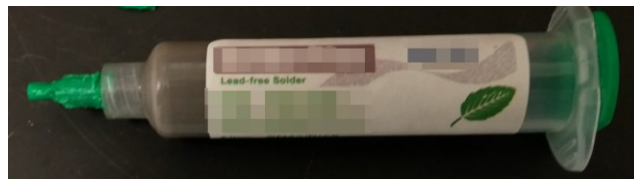


Figure 3.14 - Solder paste used to connect the wires to the strain gauges.

This solder paste could be used with the temperature of 145°C. Even though this temperature was higher than the PET's limited temperature, it was observed that PET paper could withstand this temperature without melting. Thus, this solder paste was used for all subsequent PSGs.

3.3.2. Four points bending test

- Quarter-bridge

Even though the Half-bridge was chosen for the design, Quarter-bridge was used to evaluate the conductive PSG and to determine its gauge factor first. The advantage of the Quarter-bridge was that it could be balanced using potentiometers. Due to the high resistances of the resistive PSGs, their resistances were determined directly using the Half-bridge, which would be discussed in the next section. The conductive PSG was attached on the top of the 4 points bending specimen, and it was connected to a handmade circuit with 3 potentiometers to form a completed Quarter Wheatstone bridge. The conductive PSG circuit was supplied with a current of 40

μA from the Keithley current supplier. The current excitation reduced the connections noise to compensate for weak strain gauge's signals. The voltage output from the handmade circuit was connected to the **isolated strain gauge input SCM5B38** where the signal was filtered and amplified before it went to the DAQ and the computer.

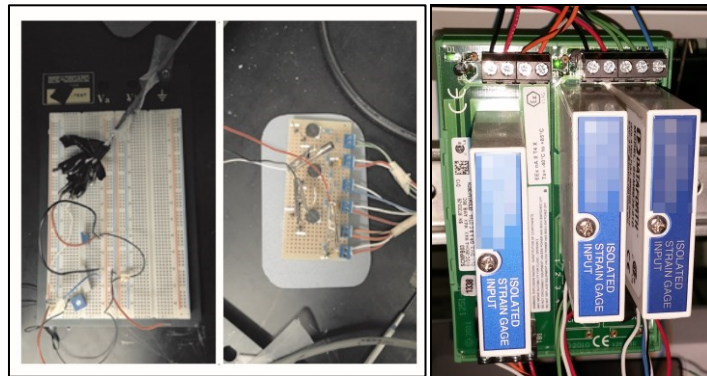


Figure 3.15 - Circuit for PSG (left), and circuit for RSG (middle), and the Isolated Strain Gauge Input (right).

The RSG in the experiment was supplied by Micro-Measurements. It had the resistance of $350\ \Omega$, and the gauge factor of 2.15. The RSG was installed on the back of the specimen. Similar to PSG, RSG was connected to a handmade circuit to complete the Wheatstone bridge. Since the RSG circuit was optimized to be used with voltage excitation, the voltage of 3.29 V was used. The voltages outputs from both circuits went to the isolated strain gauge input which filtered, isolated, amplified, and converted the signal to a high-level analog voltage output. The conditions for both PSG and RSG are summarized as below

Table 3-1: Comparison between Conductive PSG and RSG

	Conductive PSG	RSG
Power Supplier	Current Supplier of $40\ \mu\text{A}$	Voltage Supplier 3.29V
Resistance (Ω)	240.66	350
Gain	1000	1000
Gauge Factor	N/A	2.15
Position on Specimen	Top	Bottom

Specimen Dimension	1.8" x 12" x 0.12" (45.5 mm x 330 mm x 3.1 mm)
---------------------------	---

The setup for this configuration is as below

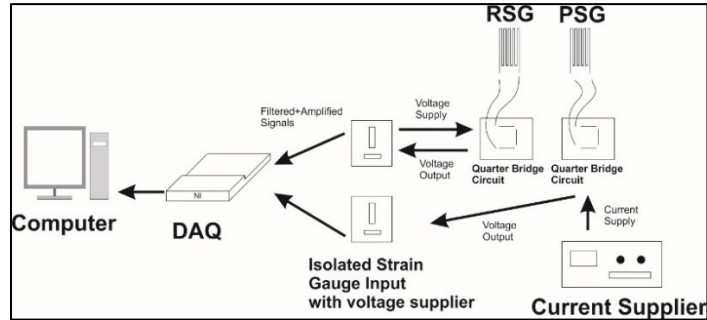


Figure 3.16 - Four points bending test setup.

Four points bending system was controlled by the Date Acquisition System (DAQ) from National Instrument. The lower rig of the 4 points bending system was controlled by a step motor so that it moved up first, then it moved down. Due to the limited downward displacement, the study only focused on the upward movement of the lower rig. While the lower rig moved upward, the load cell recorded the load that the specimen is experiencing.

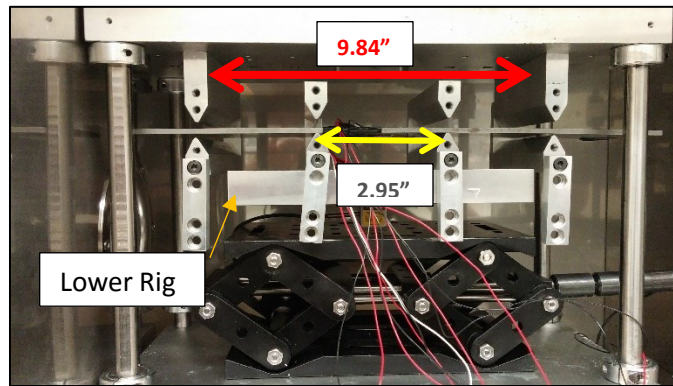


Figure 3.17 - Test specimen with PSG on top and RSG on the back. The lower rig would move up, and it was controlled by a computer.

The result for this study is showed in figure 3.18.

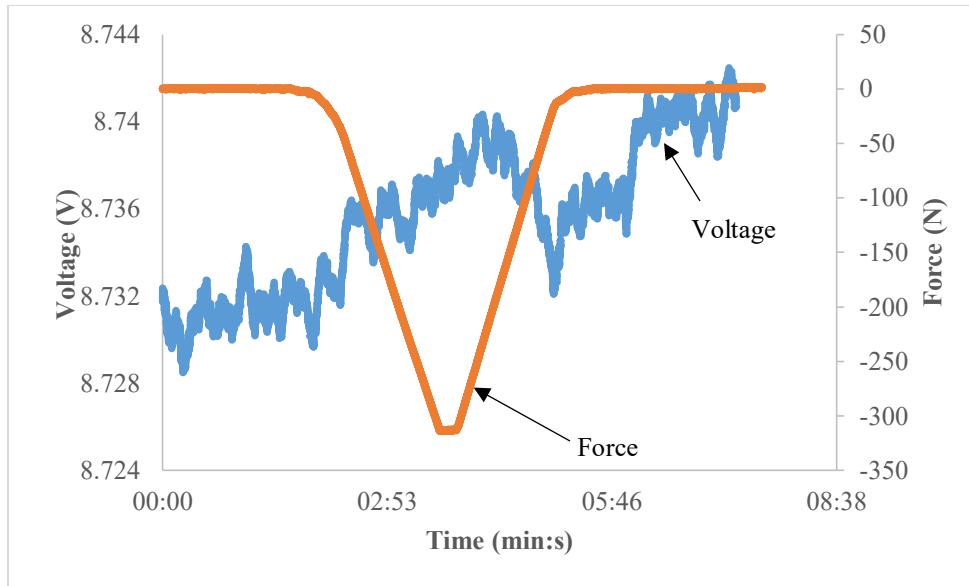


Figure 3.18 - Voltage output from the conductive PSG connected in the Quarter-bridge configuration. The force was from the load cell under the lower rig.

As the figure 3.18 indicates, the Quarter-bridge gave weak signal compared to the noises. However, the signal became more dominant as the force increases to -150N. After this compression level, the signal was higher than the noise and the gauge factor can be calculated.

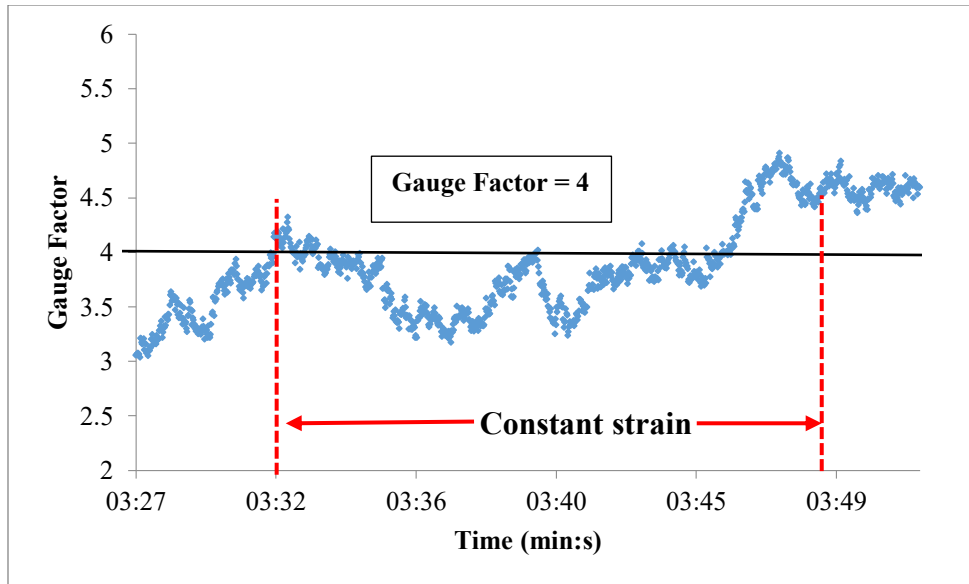


Figure 3.19 - Gauge factor of the conductive PSG. The gauge factor was averaged from 03:32 to 03:48 when the specimen was in maximum deformation.

By modifying equation 2.4, the gauge factor could be calculated in real time as in figure 3.19. Since the strain was constant when time is 03:32 to 03:48, the gauge factor was averaged from that duration and had the value of 4.0. Since the RSG was in a compression state, its voltage was inverted to represent the tension state of the PSG. The data indicates that the signal from the conductive PSG was small compared to the noise.

- Half-bridge

Even though the signal from the conductive PSG was small, the author decided to add another conductive PSG and modified the circuit to Half-bridge. The reason was to further study the ink capacity and to compare to the resistive PSG. The strain gauge's connection was as follow

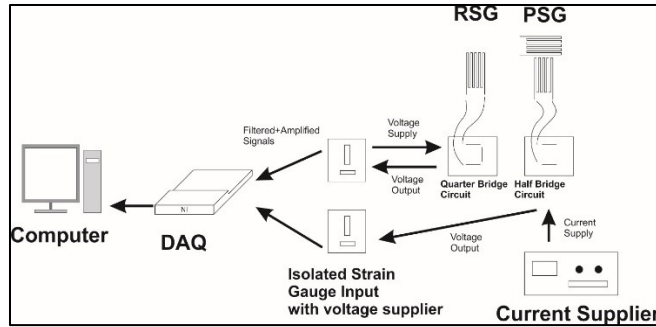


Figure 3.20 - Four points bending test setup with Half-bridge PSG installed. The RSG was in Quarter-bridge configuration.

The PSGs were used to replace the resistances R_1 and R_3 as suggested. The conditions of this test were kept the same as the conditions in the quarter-bridge test. However, the excitation current in this test was reduced to $30 \mu\text{A}$ to prevent damages to both PSGs. The strain in the Half-bridge was calculated using the equation 2.5 and with the gauge factor of 4. The result was showed below

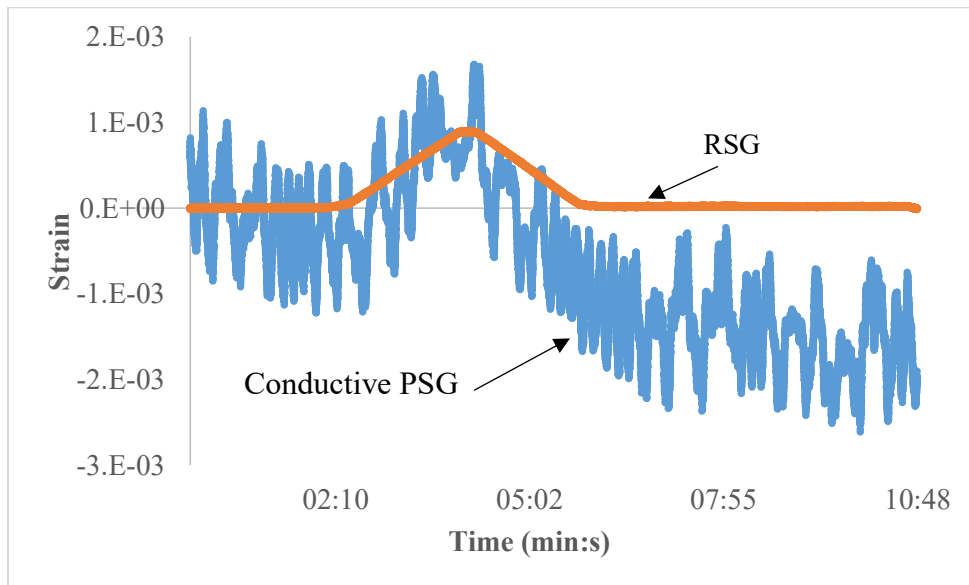


Figure 3.21 - Strain calculated from the Half-bridge formed by conductive PSG with gauge factor of 4. Notice that the strain from the RSG was inverted for comparison.

The plot showed the strains from the conductive PSG (blue) and also the RSG (orange). For comparison purpose, the strain of the RSG was inverted. As the excitation current for the conductive PSG was smaller than the excitation voltage

for the RSG, it had more noise than the RSG. However, the strain from the conductive PSG did follow the RSG's strain, which indicated that the conductive PSG was working properly. After the conductive PSGs went through tension, their strains reduced to negative (compression) values. This fact was expected to come from the viscoelastic effect of the substrate material. While the strain on the back of the substrate reduced to zero, the strain on the substrate's surface still in tension. As a result, there will be a compression stress on the surface of the substrate where the PSG locates.

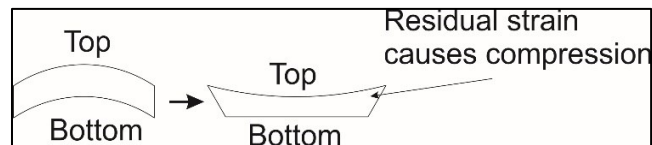


Figure 3.22 - Residual strain on the top of the substrate cause the compression.

Since this fact was due to the substrate's property, this behavior occurred in all experiment with PSGs, regardless of the strain gauge's geometry. Due to the use of the Half-bridge, the signal in this test was significantly improved from the Quarter-bridge test. However, the noise in this test was still high comparing to the signal. Thus, the conductive PSG could not be used as the sensing element for the smart membrane.

After that, the conductive PSGs were replaced by the resistive PSGs and the similar procedure was carried out to find the gauge factor of the resistive PSG.



Figure 3.23 - Resistive PSGs installed on the four points bending specimens.

Due to the high resistances of the resistive PSGs, it was more convenient to use other resistive PSGs to complete the Wheatstone bridge instead of using the potentiometers. Also, due to the limited availability of the resistive PSGs, only the Half-bridge was tested. This bridge was used to find the gauge factor of the resistive PSG based on the equation 2.5. The setup was similar to the conductive PSG in figure 3.20, but the Isolate Strain Gauge Input was not used because the high offset voltage would exceed the DAQ's range if it is amplified. In addition, the resistive PSG could only sustain the supply current of $0.9 \mu\text{A}$. The gauge factor of this strain gauge was calculated and plotted as a function of time as below

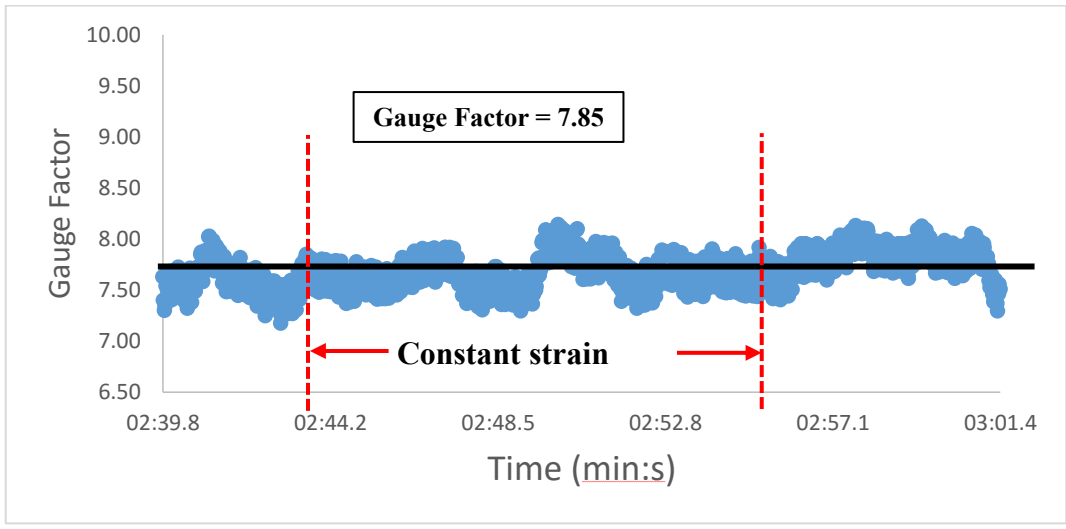


Figure 3.24 - Gauge factor of the resistive PSG. The gauge factor was averaged from 02:43 to 02:53 when the specimen was in maximum deformation.

The gauge factor was 7.85, and it was calculated based on averaging values from 02:43 to 02:53. This was the period where applied force was kept constant and the strain, subsequently, was constant. Using this gauge factor, the strain from the resistive PSG was calculated based on the equation 2.5. The result was plotted against the reference strain gauge as below

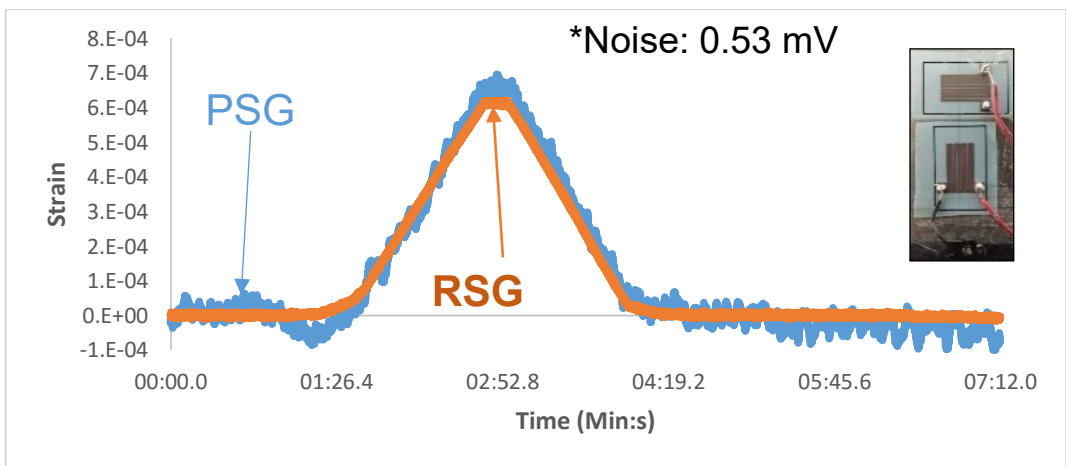


Figure 3.25 - The strain from the resistive PSG and the strain from the RSG. Notice that the strain in RSG is inverted for comparison.

For comparison purpose, the strains of the reference strain gauge were inverted. In order to reduce the environmental noises, the voltage outputs were averaged every 2s. Even without the amplifier, the averaged method significantly reduced the noise and created a distinct signal. The resistive PSG was also affected by the viscoelastic effect as the conductive PSG because they were printed on the same material. However, the voltage output from the resistive PSG was more stable and accurate. Figure 3.25 also showed that resistive PSG could withstand the strain of 0.7 microstrains. In addition, five voltage measurements of the unloaded specimen were measured, and their standard deviations were averaged to find the noise signal. This value was 0.53 mV and used to calculate the S/N. The S/N was calculated based on the equation

$$S/N = 20\log\left(\frac{Signal}{Noise}\right) \quad (3.1)$$

The S/N calculated based on this formula was 31.6 dB. As a result, the resistive PSG's sensitivity could be exposed to a strain that causes the acceptable signal.

Based on the analysis, the resistive ink performed better than the conductive ink because it had higher resistance. On the other hand, conductive ink offered more conductivity and higher adhesion with the solder. As a result, the resistive ink should be used to print the main structures of the strain gauges, and the conductive ink should be used to print the conducting pad.

3.4. Optimization of the membrane

The goal of the optimization process was to create a membrane that had longest lengths for the predefined thicknesses. Since the smart membranes were expected to be similar to the protective wraps, their thicknesses, and elastic modulus should be the same. The common protective wraps in the industry had the thicknesses of 0.03" to 0.05" (30 mils to 50 mils). They were made from Low-Density Polyethylene which had an elastic modulus of 13 ksi. Thus, the optimization process should base on this information. Also, the membrane should be able to detect the 1 lb leak product with the S/N of 30 dB. Due to the high flow rate in the pipeline, it would take less than one second for the leak substance of 1 lb to accumulate [4]. As

a result, those dimensions increased the economics of the membrane while keeping the membrane sensitive.

In the optimization, the length was increased from 11.8” to 102.4” while the thickness was increased from 0.03” to 0.05”. At each length and thickness, a force of 1 lb was distributed along the length of the membrane. The changes in the voltage of the sensor were recorded. In addition, the max Von-mises stress of the membrane was also recorded. This Von-mises stress should not exceed 1.36 Ksi because this is the yield strength of LDPE. The model was built based on the model in section 3.2 with the addition of the strain gauges. The membrane and pipe were modeled with Shell281 element, and the strain gauges were modeled with Solid227 and Circu124. Since the model was half Wheatstone bridge, the two strain gauges R_1 and R_3 on the membrane were modeled with Solid227 elements. The strain gauges R_2 and R_4 were replaced by the elements Circu124. This setup was preferred because it reduced the model complexity, which came from the thin PSG comparing to its other geometries. Notice that the current ANSYS APDL version did not have the coupling shell element, thus, solid coupling element was used to model PSG. Due to the addition of the sensor to the simulation model, the model size increased significantly. To reduce the complexity, the contact surfaces of the lower half of the membrane, where the membrane and the pipe were not in contact, were deactivated. For the excitation current, the current of $0.5 \mu\text{A}$ was applied at the node between R_1 and R_4 .

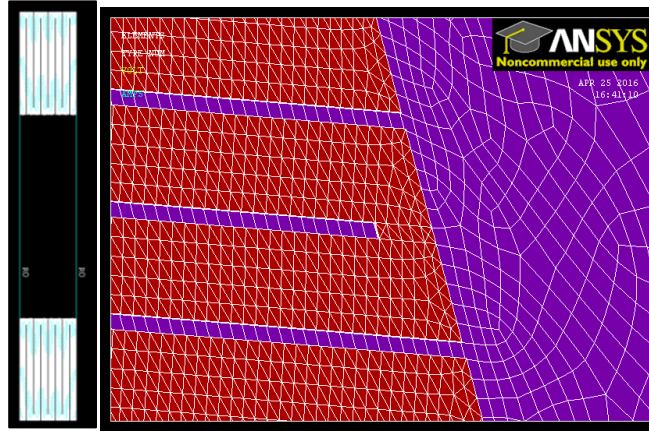


Figure 3.26 - (Left) Elements Circu124 connect the two meshed strain gauges. (Right) The connection between strain gauges' elements (red) and membrane's elements (violet).

The voltage of 0 V was applied at the node located between R₂ and R₃ to replicate the electrical constraint. Due to the conductive mechanism of the conductive and resistive inks, their material properties were assumed to be the same as the membrane's material property in the simulation. Thus, the elastic modulus and poisson ratio of the membrane and strain gauges were 13 kips and 0.3, respectively.

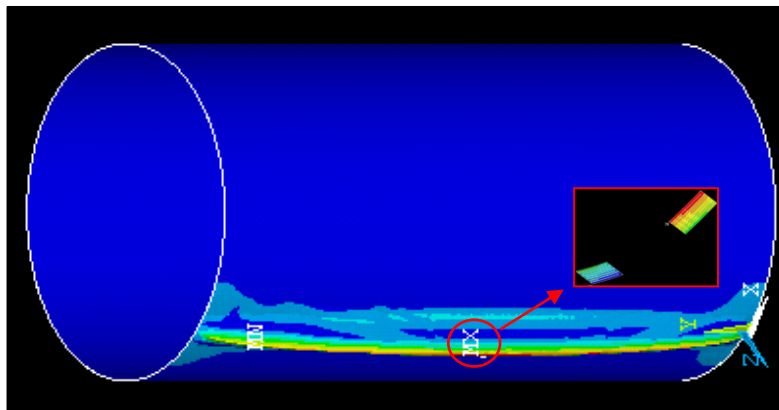


Figure 3.27 - The stress distribution on the membrane. The figure also showed voltage distribution in the strain gauges (the deformation was exaggerated).

Figure 3.27 showed the stress distribution in the membrane as the leak pressure was applied. The max Von-mises stress was calculated to be 85.6 psi, and it occurred in

the middle of the membrane. The voltage distribution in the deformed strain gauges was also continuous and as predicted.

The voltage outputs from the sensors as the length and thickness varied were plotted on the same surface plot.

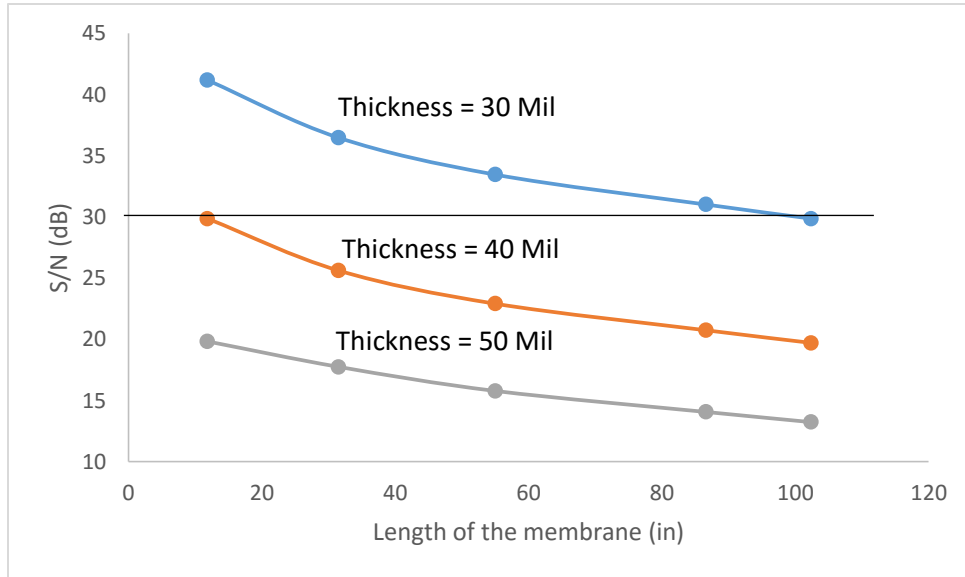


Figure 3.28 - The S/N varies with thickness and length of the membrane. The S/N of the sensor decreased as the membrane’s length and thickness increased.

The S/N in figure 3.28 was calculated using equation 3.1 with the signal voltage came from the simulation, and the noise came from the four points bending specimen. In order for the membrane to be economically competitive, its length had to be longest, and its thickness had to be thinnest. Also, the strain gauges in the 4 points bending test were tested up to the strain of 0.7 microstrains, so the Von-mises strain in the simulated strain gauges should not exceed this value. Based on this information, the membrane length should be 102”, and the thickness of 0.03” so that the membrane would have longest length and acceptable thickness. This geometry resulted in the S/N of 31 dB when 1 lb of leak substance was released. In addition, the strain at the sensor’s location could be predicted using the equation 3.2

$$\varepsilon = \frac{2V_{ba}}{I_{exR} * GF \left(1 - \frac{V_{ba}}{I_{exR}} \right)} \quad (3.2)$$

3.5. References

- [1] ANSYS, "Contact Technology Guide," ANSYS Inc., Canonsburg, 2009.
- [2] G. Carbone et al., "Contact Mechanics and Rubber Friction for Randomly Rough Surfaces with Anisotropic Statistical Properties," *The European Physical Journal E*, vol. 29, pp. 275-284, 2009.
- [3] S. S. Bhore, "Formulation and Evaluation of Resistive Inks for Applications in Printed Electronics," M.S. thesis, Dept. Chem. and Paper Eng., Western Michigan Univ., Michigan, 2013.
- [3] Trans Canada, "Application of TransCanada Keystone pipeline, L.P. for a presidential permit Authorizing the construction, connection, operation, and maintenance of pipeline facilities for the importation of crude oil to be located at the United States-Canada border," *U.S.A Department of State*.

Chapter 4: Evaluation of the membrane prototype

After designing the membrane, a prototype was created. The strain gauge in this prototype was positioned perpendicular to the other because of the small size of the testing rig and also the membrane's quality. Since the purpose of the dimple test was to demonstrate the workability of the prototype, this specimen was adequate. In this test, the prototype membrane would experience a pressure representing the leaked product's weight. This pressure was applied in the form of displacement on the membrane. The reason for applying displacement instead of applying pressure was to control the strain in the membrane. Since the prototype's material was different from the FEA smart membrane's material, only the strain control method could correlate those two membranes.

The dimple test system consisted of a 0.6" x 0.6" frame that clamped all four membrane's edges. A dimple head applied a vertical displacement, i.e. perturbation, on the membrane. In this test, the perturbation, Δd , was defined as the amount of penetration caused by the dimple head on the membrane. In addition, the voltage outputs from the sensor were converted to the changes of the equivalent resistances by dividing by the excitation current, and the results were compared to the simulation data. The disadvantage of this test was that its boundary conditions were not similar to the real loading conditions. However, this disadvantage was unavoidable due to the printing capacity of the low-cost printer.

4.1. Simulation Setup

The simulation model was created similar to the optimization model. The cylinder membrane was modified to a square membrane similar to the prototype. In order to simulate the clamping effect as in the experiment, the displacements, and rotations of all edge's nodes were fixed. The perturbation ranges from 0" to 0.175" with the increment of 0.025", and it was applied on a circular region whose diameter was 0.079" and located at the similar location as in the experiment. By applying the perturbation, i.e. strain control method, the material property of the membrane

would not become a factor affecting the design. This fact meant that if other membranes were used, the results should be similar.

4.2. Dimple Test Setup

The dimple test was carried out to evaluate the accuracy of the FEA model so that it could be used to optimize smart membrane's design. The test system was incorporated into the 6-axis testing system. The frame and the dimple head were made using rapid prototype and fixed on top of the 6-axis machine.

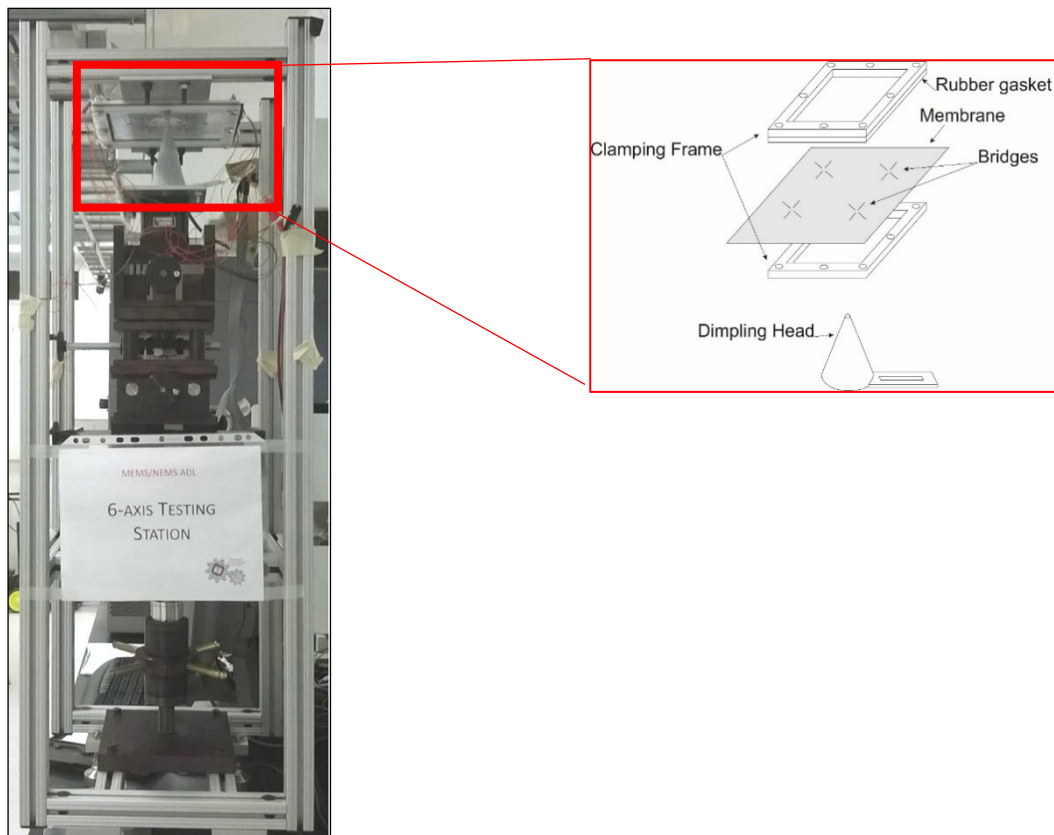
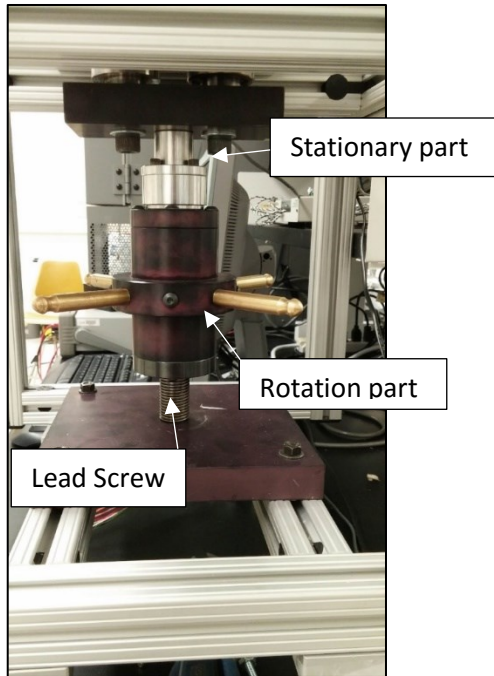
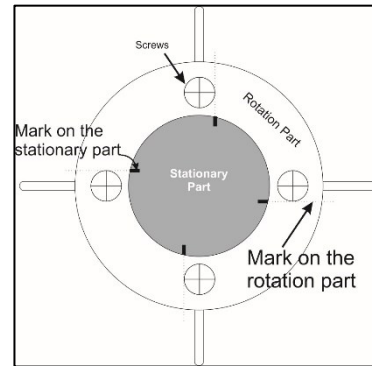


Figure 4.1 - 6 Axis Testing System with Dimple Test rig installed on top.

The perturbation was controlled by rotating the handle at the base of the testing rig. The lead screw in the machine had Pitch of 0.1" and Start of 1, thus its lead was 0.1" or 2.54 mm. By marking 4 alignment marks on the rotation and stationary parts as in figure 4.2 (b), it was practical to increase or decrease the perturbation with the increment of 0.025" or 0.635 mm.



(a)



(b) Top-view

Figure 4.2- (a) Handle that controlled the perturbation. (b) The locations of the marks used to control the amount of perturbation.

In order to validate this testing method, the rotational part was rotated, and the perturbation was measured with a digital caliper. The recorded perturbations were plotted against the expected perturbations, and the experiment was repeated 5 times for a statistical purpose.

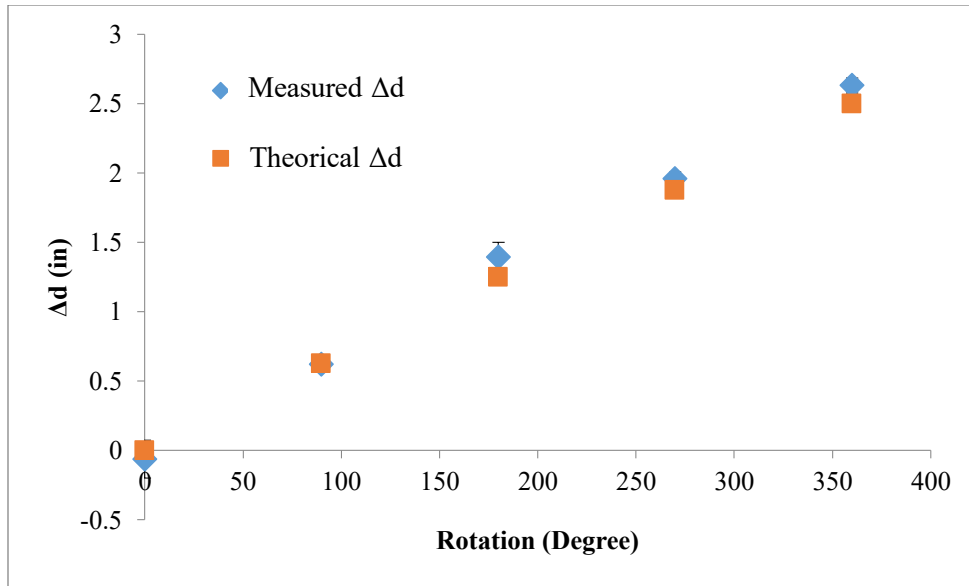


Figure 4.3 - The measured perturbations compare to the theoretical perturbations. The measured perturbation was measured using the digital caliper.

The highest standard deviation in this measurements was 0.02". The average error by using this controlling method was 8.5%. This error came from the misalignment of the marks and the backlash of the screw.

The printed sample was prepared using CorelDraw X7. The blue color printed conductive ink, and yellow color printed the resistive ink. Multiple perturbation points with known locations were pre-printed on the specimen. The sample was printed on the PET paper with the dimensions as showed below

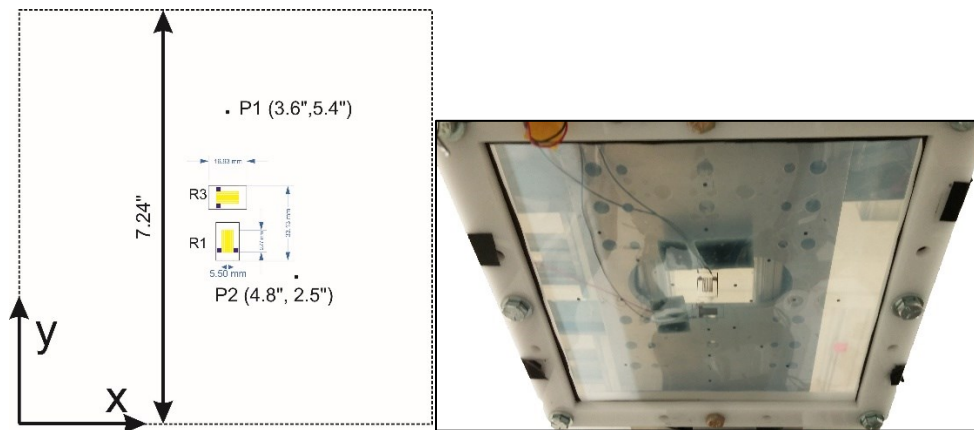


Figure 4.4 - (Left) Sample of dimple test with PSG, and its dimensions are in inches. (Right) An actual prototype was installed on the dimple test rig.

Due to the high resistance of the resistive PSGs, the other resistive PSGs were used to complete the half Wheatstone bridge. Since the R_1 and R_3 were printed vertically and horizontally, respectively, their resistances were different. To balance the bridge, R_2 is chosen so that its resistance was similar to R_3 , and R_4 was chosen so that its resistance was similar to R_1 . The resistances of those PSGs were summarized in table below

Table 4-1: Resistance of each printed strain gauge in the Wheatstone bridge circuit.

PSG	Resistance
R_1	24 M Ω
R_2	18 M Ω
R_3	17 M Ω
R_4	24 M Ω

In order to keep the membrane flattened during the installation procedure, it was slightly stretched out using electrical tape along its edges. The current supply in this experiment was set to 0.5 μ A, and the voltage output was connected directly to the DAQ before going to the computer. Notice that the supply current in the dimple test was lower than the four points bending test to keep the strain gauge safe. These currents were determined arbitrarily based on the strain gauge's capacity. A digital Low-Pass Filter with the cut-off frequency of 10 Hz was also applied to the signal to reduce the environmental noise. The setup was showed below

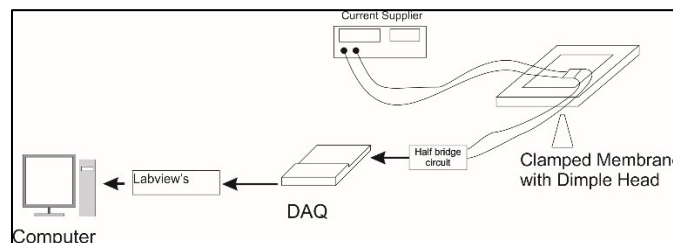


Figure 4.5 - The setup for the dimple test.

The voltage output from the experiment was divided by the supplied current to calculate the equivalent resistance's change, ΔR_{evq} . The data was plotted in figure 4.6

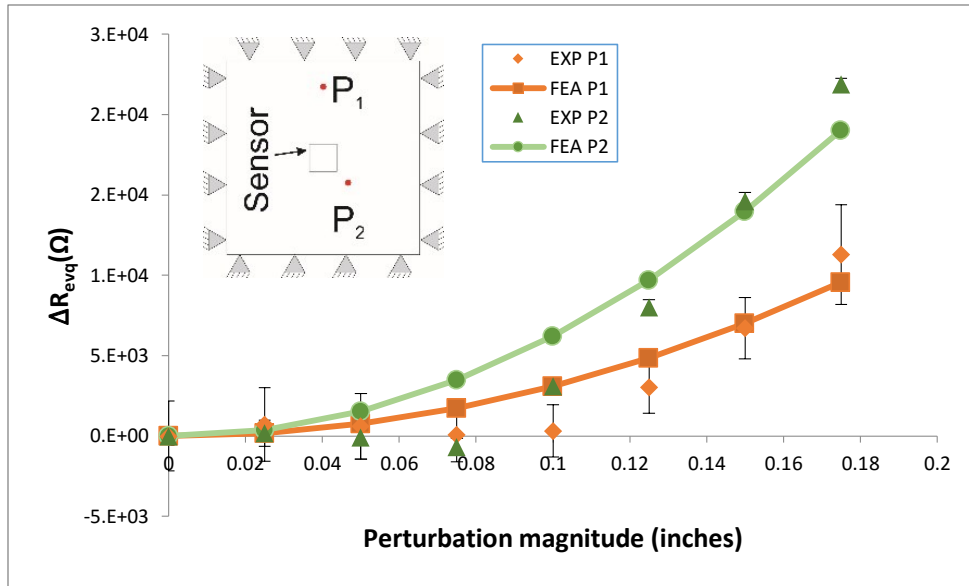


Figure 4.6 - The higher and closer the perturbation is, the higher the change in the resistance of the sensor. The experimental data do not follow simulation data because of the wrinkling membrane.

The error bars constructed in figure 4.6 were the summation of the average standard deviation from the 5 repeated measurements and the errors from the method of applying the perturbation. The data indicated that the sensor first went through compression, therefore, there are a “dip” at Δd of 0.05”. This phenomenon happened because the membrane wrinkled. As the dimple head pushed the membrane upward, it flattened that region and made sensor’s region compressed. The wrinkling membrane also reduced the effect of the Poisson strain gauge on the voltage output and the equivalent resistance. Thus, the experiment curves on figure 4.6 overshoot the simulation curves. To improve the accuracy of the dimple test, it was suggested that more initial strain was applied on the membrane to stretch it out.

4.3. References

- [1] S. Edson et al., "Finite Element Simulation of Inkjet Printed Strain Gage on Polyimide Substrates Applied to Flexible Boards," in *11th Electronics Packaging Technology Conference*, 2009.

Chapter 5: Conclusion and Future Works

5.1. Conclusion

Despite the fact that pipelines are the most efficient method to transport liquid and gas, the public maintains high resistances against their development. The reason is that pipeline's leaks pose great threats to the environment and public health. Pipeline operators have incorporated numerous methods to detect the leaks at their early states to minimize the damages. However, the current technologies are not sophisticated. This research suggests a better LDS that will detect pinhole leak as they occur. This low-cost system can be easily incorporated into the existing pipeline to detect pinhole leaks in less than a minute.

The research in this paper could be divided into two parts, manufacturing the sensor and designing the smart membrane. The author had successfully printed the strain gauges that were more sensitive and inexpensive comparing to the regular strain gauges. The strain gauges were evaluated in the four points bending test, and the resistive strain gauges performed better than the conductive strain gauges. The disadvantage of the printing process was the inconsistency of the strain gauges. This problem could be resolved by using the specialize printers. On the other hand, the optimization process was carried out to find the appropriate membrane's length and thickness. This study can be used to determine the lengths and thicknesses of membranes that wrap around all 36" pipe. From the study, the author suggests that the membrane should have the length of 102" and thickness of 0.03" (30 mils). This configuration will result in the acceptable signal when pinhole leak occurs. With the high flow rate in the pipeline, the smart membrane can detect pinhole leaks in less than a second after the leaks occur. Another sensor should be located next to the main sensor to add redundancy to the system.

Finally, a prototype of the membrane was created and evaluated in the dimple test. The result of this test was also compared to the result of the simulation, and they were similar. This fact indicated that the prototype behaved predictably. The disadvantage of the dimple test was that it could not hold the membrane properly.

Even with initial strain applied, the membrane was wrinkled. The dimple test needs to be improved in order to use as a standard test to evaluate different prototypes.

5.2. Future works

The works in this thesis create a solid foundation for the smart membrane to be developed. In order to commercialize the smart membrane, more works are needed on the manufacturing side and data acquisition system. Possible extensions of this research include, and are not limited to the following:

- The Direct to Garment (DTG) printer which specializes in printing electronics should be used to manufacture the membrane. This type of printer allows printing on any membrane's materials and membrane's sizes. A feeding system should also be developed to move the membrane across the printer.
- The data acquisition system should be developed for the membrane. The system was expected to detect the change of at least 0.01 V from the membrane. This system should be capable of sending signals wirelessly to the central station where they are evaluated for unexpected changes.
- Design a better way to connect the circuit on the membrane. The sensors connection currently are connected by soldering. This method will limit the performances of the sensors.
- The metal frame should be used for the dimple test so that higher initial strain could be applied on the prototype. Moreover, the dimple head should be controlled by the computer to reduce human error.

References

- [1] CEPA, Liquids Pipeline [Online]. Available: <http://www.cepa.com/about-pipelines/types-of-pipelines/liquids-pipelines>.
- [2] C. Kelly. (2013). Enbridge Cleanup May Cost \$1-billion, Company Warns [Online]. Available: <http://www.theglobeandmail.com/globe-investor/enbridge-cleanup-may-cost-1-billion-company-warns/article10041757/>.
- [3] Reuters. (2012). Update 2-Enbridge Fined \$3.7 Mln for 2010 US Oil Spill [Online]. Available: <http://www.reuters.com/article/enbridge-spill-fine-idUSL2E8I2DTH20120703>.
- [4] R. Fletcher, and J. V. Reet, Pipeline Rules of Thumb Handbook: A Manual of Quick, Accurate Solutions to Everyday Pipeline Engineering Problems, 7th ed., Amsterdam: Gulf Professional Publishing, 2009, pp. 605-614.
- [5] EUB, "Pipeline Performance in Alberta, 1990-2005," Alberta Energy and Utilities Board, Calgary, 2007.
- [6] C. Cheng, "Evaluation of Pipeline Leak Detection Technologies," M.Eng. thesis. Dept. Mech. Eng., University of Alberta, Edmonton, 2013.
- [7] A. Swift. (2011). The Keystone XL Tar Sands Pipeline Leak Detection System Would Have Likely Missed the 63,000 Gallon Norman Wells Pipeline Spill [Online]. Available: <https://www.nrdc.org/experts/anthony-swift/keystone-xl-tar-sands-pipeline-leak-detection-system-would-have-likely-missed>
- [8] L. Song. (2012). Few Oil Pipeline Spills Detected by Much-Touted Technology [Online]. Available: <http://insideclimatenews.org/news/20120919/few-oil-pipeline-spills-detected-much-touted-technology>.

- [9] A. Jager A. et al., "Investigation on Strain Gauges Made from Carbon Black Based Ink," in AMA Conferences. 2015.
- [1] CEPA, *Liquids Pipeline* [Online]. Available: <http://www.cepa.com/about-pipelines/types-of-pipelines/liquids-pipelines>. [Accessed 31 March 2016].
- [2] Alyeska Pipeline Service Company, *Pipeline Facts* [Online]. Available: <http://www.alyeska-pipe.com/TAPS/PipelineFacts>. [Accessed 02 April 2016].
- [3] L. Song. (2012). *Few Oil Pipeline Spills Detected by Much-Touted Technology* [Online]. Available: <http://insideclimatenews.org/news/20120919/few-oil-pipeline-spills-detected-much-touted-technology>. [Accessed 30 June 2015].
- [4] C. Cheng, "Evaluation of Pipeline Leak Detection Technologies," M.Eng. thesis. Dept. Mech. Eng., University of Alberta, Edmonton, 2013.
- [5] International Association of Oil & Gas Producers, "Risk Assessment Data Directory- Summary". OGP, 2010.
- [6] Committee on the Safety of Marine Pipelines et al., "Maintaining the Integrity of the Marine Pipeline Network," in *Improving the Safety of Marine Pipelines*. Washington, D.C., National Academy Press, 1994, pp. 45.
- [7] A. Swift. 2011. *The Keystone XL Tar Sands Pipeline Leak Detection System Would Have Likely Missed the 63,000 Gallon Norman Wells Pipeline Spill* [Online]. Available: <https://www.nrdc.org/experts/anthony-swift/keystone-xl-tar-sands-pipeline-leak-detection-system-would-have-likely-missed>
- [8] D. Shaw et al., "Leak Detection Study - DTPH56-11-D-000001," U.S. Department of Transportation Pipeline and Hazardous Materials Safety Administration, Worthington, 2012.

- [9] D. Mawhinney. (2015). *Corrosion Pit* [Online]. Available: https://en.wikipedia.org/wiki/Pitting_corrosion#/media/File:Corrosion.Pit.jpg.
- [10] Alaska Department of Environmental Conservation, "Technical Review of Leak Detection Technologies," Alaska Department of Environmental Conservation.
- [11] J. Zhang et al., "Review of Pipeline Leak Detection Technologies," Pipeline Simulation Interest Group, Prague, 2013.
- [12] J. Summa, "Pipeline Leak Detection Operational Improvements: An Overview of Currently Available Leak Detection Technologies & US Regulations/Standards," in *6th Pipeline Technology Conference*, Hannover, 2011.
- [13] G. Geiger, "State-of-the-Art in Leak Detection and Localization," in *Pipeline Technology 2006 Conference*, Germany, 2006.
- [14] P. Siebenaler et al., *Detection of Small Leaks in Liquid Pipelines: Gap Study of Available Methods (PL-1)*, Southwest Research Institute, 2007.
- [15] J. C. Liou, and L. Cui, T. Li, "Hazardous Liquid Leak Detection Techniques and Processes," General Physics Corp., 2003.
- [16] Integrity Diagnostics, "Introduction to Acoustic Emission [Online]. Available: http://www.idinspections.com/?page_id=126. [Accessed 26 May 2013].
- [17] R. K. Miller et al., *A Reference Standard for the Development of Acoustic Emission Pipeline Leak Detection Techniques*, NDR&E International, pp. 32, 1999.
- [18] Y. Gao, "A Model of the Correlation Function of Leak Noise in Buried Plastic Pipes." *Journal of Sound and Vibration*, pp. 133-148, 2004.

- [19] J. Zhang, "Statistical Pipeline Leak Detection for All Operating Conditions," *Pipeline & Gas Journal*, vol. 2, pp. 42-45, 2001.
- [20] G. Hessel, "A Neural-network Approach for Acoustic Leak Monitoring in Pressurized Plants with Complicated Topologies," *Control Engineering Practice*, vol. 4, no. 9, pp. 1271-1276, 1996.
- [21] H. Dasilva, et al., "Leak Detection in Petroleum Pipelines Using a Fuzzy System," *Journal of Petroleum Science and Engineering*, vol. 49, no. 3-4, pp. 223-238, 2005.
- [22] P. Lee et al., "Leak Location Using the Pattern of the Frequency Response Diagram in Pipelines: A Numerical Study," *Journal of Sound and Vibration*, pp. 1051-1073, 2005.
- [23] J. Hu, et al., "Detection of Small Leakage from Long Transportation Pipeline with Complex Noise," *Journal of Loss Prevention in the Process Industries*, vol. 24, pp. 449-457, 2011.
- [24] E. Rochatm, and M. Nikles, "Fiber Optic Asset Integrity Monitoring Using Brillouin-Based Distributed Sensing for the Oil and Gas and Energy Industry: Challenges and Achievements," in *Proceedings of the 22nd International Conference on Optical Fiber Sensors*, 2012.
- [25] D. Inaudi, R. et al., "Detection and Localization of Micro-Leakages using Distributed Fiver Optic Sensing," in *7th International Pipeline Conference*, 2008.
- [26] D. Inaudi, and B. Glisic, "Long-Range Pipeline Monitoring by Distributed Fiber Optic Sensing," *Journal of Pressure Vessel Technology*, vol. 132, 2010.
- [27] Process Online, *Digital Pipeline Leak Detection* [Online]. Available: <http://www.processonline.com.au/articles/29927-Digital-pipeline-leak-detection-using-fibre-optic-distributed-temperature-sensing>. [Accessed 26 June 2013].

- [28] C. Apps et al., "Evaluation of Distributed Leak Detection Technologies for Liquid Pipeline," in *C-Fer Technologies*, Edmonton, 2012.
- [29] S. Chet et al., "The Application of a Continuous Leak Detection System to Pipelines and Associated Equipment," *IEEE*, pp. 900-906, 1989.
- [30] D. Atherton, and L. Clapham, *In-Line Inspection Tools for Pipelines* [Online]. Available: <http://www.physics.queensu.ca/~amg/expertise/inline.html>. [Accessed 03 April 2016].
- [31] M. Beller, "Pipeline Inspection Utilizing Ultrasound Technology on the Issue of Resolution," *Pigging Products and Services Association*, 2007.
- [32] H. R., "Smart Pigging Philosophy," in *The NACE International Annual Conference and Exposition*, Concord, 1996.
- [33] T. Chris, "Pipeline Leak Detection Techniques," *Annual Computer Science Series*, 2007.
- [34] A. Afifi et al., "Pressure Point Analysis for Early Detection System," *IEEE*, 2011.
- [35] Krohne Inc., *PipePatrol-Pipeline Leak Detection* [Online]. Available: <http://krohne.com/en/products/systems/pipepatrol/>
- [36] API, "Computational Pipeline Monitoring for Liquid Pipelines: Pipeline Segment," *American Petroleum Institute*, 2007.
- [37] C. Silva, *Vibration Monitoring, Testing, and Instrumentation*, Canada: CRC Press, 2007.
- [38] Measurements Group, "Wheatstone Bridge Nonlinearity," Measurement Group, 2000.
- [39] Micro-Measurements, "Errors Due to Wheatstone Bridge Nonlinearity," Micro-Measurements, 2010.

- [40] Micro-Measurements, "Strain Gage Thermal Output and Gauge Factor Variation with Temperature," Micro-Measurements, 2014.
- [41] K. Hoffmann, "Applying the Wheatstone Bridge Circuit," HBM.
- [42] Vishay Precision, "Errors Due to Wheatstone Bridge Nonlinearity," Vishay Precision Group.
- [43] N. D. Sankir, "Flexible Electronics: Materials and Device Fabrication," Ph.D. dissertation. Mat. Sc. Eng., Virginia Polytechnic Institute and State Univ., Blacksburg, VA, 2005.
- [44] S. S. Bhore, "Formulation and Evaluation of Resistive Inks for Applications in Printed Electronics," M.S. thesis, Dept. Chem. and Paper Eng., Western Michigan Univ., Michigan, 2013.
- [45] The U.S. Department of Transportation, "Leak Detection Technology Study," The U.S. Department of Transportation, 2007.
- [46] PTC, "Reliable and Cost Effective Leak Detection with a New Generation of Ultrasonic PIGs," in *7th Pipeline Technology Conference 2012*, 2012.
- [47] B. Andò, "All-Inkjet Printed Strain Sensors," *IEEE*, vol. 13, no. 12, pp. 4874-4879, 2013.
- [48] ICF International, "North American Midstream Infrastructure through 2035: Capitalizing on Our Energy Abundance". INGAA Foundation, Washington, D.C., 2014.
- [49] AOPL and API. *Pipeline 101* [Online]. Available: <http://www.pipeline101.org>.
- [50] G.A.O., "Pipeline Safety, "U.S. Govt. Accountability Office: Collecting Data and Sharing Information on Federally Unregulated Gathering Pipelines Could Help Enhance Safety, Washington, D.C., 2012.
- [51] Argonne National Laboratory, "Natural Gas Pipeline Technology Overview," U.S. Dept. of Energy, Oak Ridge, TN, 2007.

- [52] INGAA, "Interstate Natural Gas Pipeline Desk Reference," INGAA, 2009.
- [53] P. W. Parfomak, "Keeping America's Pipelines Safe and Secure: Key Issues for Congress," Congressional Research Service, 2013.
- [54] INGAA Foundation, "Building Interstate Natural Gas Transmission Pipelines: A Primer," INGAA, 2013.
- [55] T. E. Bell. (2015). *Pipelines Safety and Security: Is It No More Than a pipe Deam?* [Online]. Available:
<http://www.tbp.org/pubs/Features/W15Bell.pdf>.
- [56] Azh7. *The World's Longest Ammonia Pipeline from Russia to Ukraine*. [Online]. Available:
https://en.wikipedia.org/wiki/Pipeline_transport#/media/File:Ammiakoprovod_NS.jpg
- [57] Bryan, *Close Up Pictures of Gas Line Explosion Damage Taken from the Intersection of Glenview Dr. & Earl Ave., Facing South on Glenview Dr., in San Bruno, CA*. [Online]. Available:
https://en.wikipedia.org/wiki/2010_San_Bruno_pipeline_explosion#/media/File:Pipe-from-Sanbruno-explosion.jpg
- [1] ANSYS, "Contact Technology Guide," ANSYS Inc., Canonsburg, 2009.
- [2] G. Carbone et al., "Contact Mechanics and Rubber Friction for Randomly Rough Surfaces with Anisotropic Statistical Properties," *The European Physical Journal E*, vol. 29, pp. 275-284, 2009.
- [3] S. S. Bhore, "Formulation and Evaluation of Resistive Inks for Applications in Printed Electronics," M.S. thesis, Dept. Chem. and Paper Eng., Western Michigan Univ., Michigan, 2013.
- [3] Trans Canada, "Application of TransCanada Keystone pipeline, L.P. for a presidential permit Authorizing the construction, connection, operation, and

maintenance of pipeline facilities for the importation of crude oil to be located at the United States-Canada border," *U.S.A Department of State*.

- [1] S. Edson et al., "Finite Element Simulation of Inkjet Printed Strain Gage on Polyimide Substrates Applied to Flexible Boards," in *11th Electronics Packaging Technology Conference*, 2009.

Appendix: Simulation Appendix

Introduction

The simulation in this thesis allowed for an understanding of how the membrane's sensor respond to the different applying pressures. The simulation was performed in ANSYS Multiphysics using coupling elements and contact elements. By utilizing the command line input method, an optimization model of the membrane could be created. In this appendix, an example input file will be examined in detail. This input file was taken from the optimization procedure.

Example Input File

! Including 4 - Model 1 cells (Printed SG).

```
/CLEAR
/prep7
!
wire_length=10! [mm]
wire_width=0.6! [mm]
wire_thickness=0.01![mm]

mid_length=0.1![mm]
mid_width=0.6![mm]
mid_thickness=wire_thickness![mm]
sg_resistant=24e6
!
spec_length=12000![mm]
spec_width=2872.68![mm]
spec_thickness=5![mm]
spec_ex=13000![MPa]
spec_prxy=0.3
!
wrap_thickness=0.75
wrap_ex=90
wrap_prxy=0.3
rad_pipe=457.2
rad_wrap=457.2
!
sg_ex=wrap_ex![MPa]
sg_prxy=wrap_prxy
!
```

```

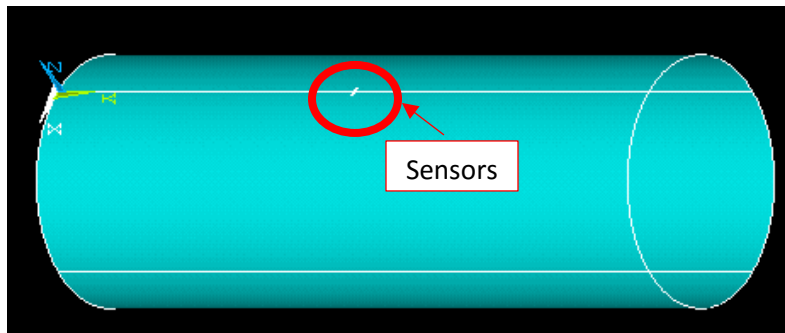
length=2400
k,1,,,-rad_wrap
k,2,,200+length,-rad_wrap
l,1,2
!
circle,1,rad_pipe,2
circle,1,rad_wrap,2
!
lsel,s,,,2,5,1
adrag,all,,,,,,,,1
!
lsel,s,,,6,9,1
adrag,all,,,,,,,,1
!
blc4,spec_width/2-5.5/2,spec_length/2-
5,wire_width,wire_length,wire_thickness*500
blc4,spec_width/2-5.5/2+0.6,spec_length/2-5+10-
0.6,mid_length,mid_width,mid_thickness*500
blc4,spec_width/2-5.5/2+0.6+mid_length,spec_length/2-
5,wire_width,wire_length,wire_thickness*500
blc4,spec_width/2-5.5/2+1.2+mid_length,spec_length/2-
5,mid_length,mid_width,mid_thickness*500
vsel,s,loc,z,0,10,1
vgen,4,all,,,2*wire_width+2*mid_length
vdele,16,,,1
vglue,all
vsel,all
vgen,2,all,,,,,
vsel,s,,,1,15,1
!
csys,0
vgen,1,all,,,30,,,,,1
csys,0
!
csys,1
allsel,all
vgen,1,all,,,90,,,,,1
csys,0
allsel,all
vgen,1,all,,,6015,-1333.6+length/2,-2.5,,,1
allsel,all
asel,u,,,1,4
btol,1e-9
aptn,all
allsel,all
vdele,all,,,1

```

```

!
allsel,all
asel,s,,195,201,1
asel,a,,211,217,1
asel,a,,443,458,1
cm,sensor_back,area
!
allsel,all
asel,u,,1,6,1
asel,u,,459,460,1
asel,u,,sensor_back
adele,all,,1
!
allsel,all
asel,s,,sensor_back
vext,all,,,,,wire_thickness
allsel,all

```



This section of the input file declares the parameters for the simulation. The parameters include geometry dimensions and material properties. First, the areas corresponding to the pipe and wrap are created. Then, the strain gauges are created on the membrane. Notice that the strain gauges are modeled with a rectangular shape that intercepts the membrane. Then, the overlap command is issued and the original strain gauges are deleted. This action will leave the imprints of the strain gauges on the circular membrane. Then, these imprints will be extruded to generate the final strain gauges.

```

! Element declaration
et,1,shell281
! Element for pipe
et,2,shell281
! Element for membrane

```

```

!keyopt,2,1,1
et,3,solid227
! Element for SGs
keyopt,3,1,101
! Piezoresistivity
et,4,circu124
keyopt,4,1,0
r,4,sg_resistant
! Material Declaration
rho=sg_resistant*0.6*wire_thickness/80
mp,ex,1,spec_ex
mp,prxy,1,spec_prxy
!
mp,ex,2,wrap_ex
mp,prxy,2,wrap_prxy
mp,mu,2,0.4
!
mp,ex,3,sg_ex
mp,prxy,3,sg_prxy
mp,rsvx,3,rho
mp,rsvy,3,rho
mp,rsvz,3,rho
!
! Mesh
vsel,all
type,3
mat,3
esize,0.13!0.13
!mshape,1,3d
vmesh,all
!
allsel,all
asel,s,,1,4,1
type,1
mat,1
sectype,1,shell
secdata,spec_thickness
secnum,1
esize,30!30
smrtsize,5,,2
amesh,all
allsel,all
!
allsel,all
asel,u,,1,4,1
aslv,u,1

```

```

asel,a,,,sensor_back
type,2
mat,2
sectype,2,shell
secdata,wrap_thickness
secnum,2
esize,30!30
smrtsize,5,,2
amesh,all
allsel,all

```

After that, the element types and their properties are declared. The strain gauge, membrane, and pipe is meshed subsequently.

```

! Connect the circuit
ksel,s,,,76
nslk,s
*get,InputPlus,node,0,num,max
!
ksel,s,,,80
nslk,s
*get,OutputMin,node,0,num,max
!
ksel,s,,,85
nslk,s
*get,InputMin,node,0,num,max
!
ksel,s,,,82
nslk,s
*get,OutputPlus,node,0,num,max
!
ksel,s,,,79
nslk,s
*get,Vb,node,0,num,max
!
ksel,s,,,83
nslk,s
*get,Va,node,0,num,max
!
allsel,all
type,4
real,4
e,OutputMin,InputMin
e,OutputPlus,InputPlus
allsel,all
!

```

```

! Apply load
lsel,s,,,24
nsl,s,
*get,node_load,node,0,count
f,all,fz,5/(node_load)
allsel,all
!asel,s,,,459,460,1
!sfa,all,,pres,-291
allsel,all
! B.C. Conditions
f,InputPlus,amps,0.4e-6
d,InputMin,volt,0

```

Then, the elements Circu124 are used to connect the strain gauges. Note that these elements are used as resistors. The electrical boundary conditions are also applied at the corresponding nodes to replicate the Half Wheatstone bridge. The applied force is also distributed along the bottom of the membrane. Applying force at this stage will not affect the contact and target elements that are generated later.

```

! Defining contact/target elements
et,6,conta174
tshap,quad8
!keyopt,6,1,0
! Selects degrees of freedom:UX, UY, UZ
!keyopt,6,2,0
! contact algorithm: Augmented Lagrangian(0)
!keyopt,6,4,0
! location of contact detection point: On Gauss points
!keyopt,6,5,2
! CNOF/ICONT automated adjustment: Reduce penetration with auto CNOF
!keyopt,6,6,1
! Contact stiffness variation: Make a nominal refinement to the allowable stiffness
range
!keyopt,6,8,0
! Asymmetric contact selection: No action
!keyopt,6,9,1
! Effect of initial penetration or gap: Exclude both initial geometrical penetration or
gap and offset
!keyopt,6,10,0
! Contact stiffness update: Each load step if FKN is redefined during load step (pair
based).
!keyopt,6,11,1
! Shell thickness effect: Include

```

```

keyopt,6,12,0
! Behavior of contact surface
R,6,,,0.001,,,
! R,id,r1,r2,FKN,FTOLN,ICONT,PINB
!RMORE,,,,,
! RMORE,PMAX,PMIN,TAUMAX,CNOF,FKOP,FKT
!RMORE,,,,,
! COHE,TCC,FHTG,SBCT,RDVF,FWGT,ECC
!RMORE,,2,1,,,
! FHEG,FACT,DC,SLTO,TNOP,TOLS,MCC
!RMORE,,,,,
! FPAT,
et,5,170
real,6
!-----
! Applying contact/target elements
asel,s,,1,4,1
nsla,s,1
type,5
real,6
esurf,,
allsel,all
!aslv,u,1
!asel,u,,1,4,1
!asel,a,,,sensor_back
asel,s,,5,6,1
nsla,s,1
type,6
real,6
esurf,,,
! Flip normal
allsel,all
esel,s,type,,6
ESURF,,REVERSE
esel,all
allsel,all

```

After that, the contact surfaces are applied on the pipe and the membrane. The membrane is used as contact surface because it is softer than the pipe, i.e. target surface. Notice that the normals for the contact elements are flipped so that they faced the target surface.

```

!-----
lsl,s,,2,9,1

```

```

nsl,s,1
d,all,ux,0
d,all,uy,0
d,all,uz,0
!
lsel,s,,10
lsel,a,,13,17,2
lsel,a,,18
lsel,a,,21,25,2
nsl,s,1
d,all,ux,0
d,all,uy,0
d,all,uz,0
!-----
!nsl,all
!d,all,ux,0
!d,all,uy,0
!d,all,uz,0
!d,all,rotx,0
!d,all,roty,0
!d,all,rotz,0
!-----
/solu
allsel,all
!nropt,full,,on
!nlgeom,on
!sstif,on
nsubst,20
!kbc,0
solve
/PREP7
UPGEOM,1,,file,rst,
/solu
solve
finish

```

The code above applies physical boundary conditions to the pipe and the membrane.

The model is solved twice so that the piezoelectric effect can be calculated.

```

/post26
*cfopen,BigModelStudy.txt,,append
!
*vwrite,'D: ',jj
(A3,F8.2)

```

```
*vwrite,'A1: ',volt(Vb),' B1: ',volt(OutputPlus)
(A5,F10.8,A5,F10.8)
*vwrite,'Vba: ',volt(Vb)-volt(OutputPlus)
(A5,F10.8)
!
*CFCLOSE
!resume
!*enddo
```

The code above is the post processing step. The output voltages are extracted and written to a text file. The difference between these voltages is the voltage output from the Wheatstone bridge.⁴